AAPT PHYSICS EDUCATION | AMERICAN JOURNAL of PHYSICS

Understanding some simple phenomena in thermoacoustics with applications to acoustical heat engines

John Wheatley, T. Hofler, G. W. Swift, and A. Migliori

Citation: American Journal of Physics **53**, 147 (1985); doi: 10.1119/1.14100
View online: http://dx.doi.org/10.1119/1.14100
View Table of Contents: http://scitation.aip.org/content/aapt/journal/ajp/53/2?ver=pdfcov
Published by the American Association of Physics Teachers

Articles you may be interested in

How to match an acoustical load to a thermoacoustic heat engine?
AIP Conf. Proc. **1573**, 1445 (2014); 10.1063/1.4860877

Understanding of thermoacoustic phenomena and their applications
AIP Conf. Proc. **1474**, 29 (2012); 10.1063/1.4749293

NonNormal Investigations of a ThermoAcoustic Heat Engine
AIP Conf. Proc. **1389**, 54 (2011); 10.1063/1.3636669

Unconventional thermoacoustic heat engines
J. Acoust. Soc. Am. **119**, 3414 (2006); 10.1121/1.4786811

An intrinsically irreversible thermoacoustic heat engine
J. Acoust. Soc. Am. **74**, 153 (1983); 10.1121/1.389624

WebAssign
Free Physics Videos
Add these videos and many more resources — free with WebAssign.
bit.do/PhysicsResources

This article is copyrighted as indicated in the article. Reuse of AAPT content is subject to the terms at: http://scitation.aip.org/termsconditions. Downloaded to IP: 95.68.109.7 On: Wed, 23 Apr 2014 04:24:23

[9]For papers dealing with the time-separation variable in bound systems, see H. Yukawa, Phys. Rev. **79**, 416 (1953); G. C. Wick, *ibid.* **96**, 1124 (1954); M. Markov, Suppl. Nuovo Cimento **3**, 760 (1956); T. Takabayasi, Nuovo Cimento **33**, 668 (1964); S. Ishida, Prog. Theor. Phys. **46**, 1570, 1905 (1971); R. P. Feynman, M. Kislinger, and F. Ravndal, Phys. Rev. D **3**, 2706 (1972); G. Preparata and N. S. Craigie, Nucl. Phys. **B102**, 478 (1976); Y. S. Kim, Phys. Rev. D **14**, 273 (1976); J. Lukierski and M. Oziewics, Phys. Lett. **69B**, 339 (1977); D. Dominici and G. Longhi, Nuovo Cimento A **42**, 235 (1977); T. Goto, Prog. Theor. Phys. **58**, 1635 (1977); H. Leutwyler and J. Stern, Phys. Lett. **73B**, 75 (1978); and Nucl. Phys. **B157**, 327 (1979); I. Fujiwara, K. Wakita, and H. Yoro, Prog. Theor. Phys. **64**, 363 (1980); J. Jersak and D. Rein, Z. Phys. C **3**, 339 (1980); I. Sogami and H. Yabuki, Phys. Lett. **94B**, 157 (1980); M. Pauri, in *Group Theoretical Methods in Physics*, Proceedings of the 9th International Colloquium, Cocoyoc, Mexico, edited by K. B. Wolf (Springer-Verlag, Berlin, 1980); G. Marchesini and E. Onofri, Nuovo Cimento A**65**, 298 (1981); E. C. G. Sudarshan, N. Mukunda, and C. C. Chiang, Phys. Rev. D **25**, 3237 (1982).
[10]For a recent pedagogical paper on this problem, see C. H. Blanchard, Am. J. Phys. **50**, 642 (1982).
[11]For a possible departure from the accepted view, see E. Prugovecki, Found. Phys. **12**, 555 (1982); Phys. Rev. Lett. **49**, 1065 (1982).
[12]E. Prugovecki, *Quantum Mechanics in Hilbert Space* (Academic, New York, 1981), 2nd ed.
[13]H. P. Robertson, Phys. Rev. **34**, 163 (1929).
[14]The word "Fourier relation" was used earlier by Blanchard in Ref. 10. This word is necessary because the energy is not a variable canonically conjugate to the time variable.
[15]G. N. Fleming, Phys. Rev. **137**, B188 (1965); G. N. Fleming, J. Math. Phys. **11**, 1959 (1966).
[16]Y. S. Kim and M. E. Noz, Am. J. Phys. **46**, 484 (1978).
[17]For some of the latest papers on hadronic mass spectra, see N. Isgur and G. Karl, Phys. Rev. D **19**, 2653 (1978); D. P. Stanley and D. Robson, Phys. Rev. Lett. **45**, 235 (1980). For review articles written for teaching purposes, see P. E. Hussar, Y. S. Kim, and M. E. Noz, Am. J. Phys. **48**, 1038 (1980); **48**, 1043 (1980).
[18]For papers dealing with form factor behavior, see K. Fujimura, T. Kobayashi, and M. Namiki, Prog. Theor. Phys. **43**, 73 (1970); R. G. Lipes, Phys. Rev. D **5**, 2849 (1972); Y. S. Kim and M. E. Noz, *ibid.* **8**, 3521 (1973).
[19]Y. S. Kim and M. E. Noz, Phys. Rev. D **15**, 335 (1977).
[20]Y. S. Kim and M. E. Noz, Am. J. Phys. **51**, 368 (1983).
[21]For papers dealing with the jet phenomenon, see T. Kitazoe and S. Hama, Phys. Rev. D **19**, 2006 (1979); Y. S. Kim, M. E. Noz, and S. H. Oh, Found. Phys. **9**, 947 (1979); T. Kitazoe and T. Morii, Phys. Rev. D **21**, 685 (1980); Nucl. Phys. **B164**, 76 (1980).
[22]E. P. Wigner, Ann. Math. **40**, 149 (1939).
[23]Y. S. Kim, M. E. Noz, and S. H. Oh, J. Math. Phys. **10**, 1341 (1979); Am. J. Phys. **47**, 892 (1979); J. Math Phys. **21**, 1224 (1980).
[24]P. A. M. Dirac, Rev. Mod. Phys. **21**, 392 (1949).
[25]D. Han and Y. S. Kim, Am. J. Phys. **49**, 1157 (1981).
[26]F. C. Rotbart, Phys. Rev. D **23**, 3078 (1981). For a physical basis for Rotbart's calculation, see L. P. Horwitz and C. Piron, Helv. Phys. Acta **46**, 316 (1973). See also Ref. 16.
[27]D. Han, M. E. Noz, and Y. S. Kim, Phys. Rev. D **25**, 1740 (1982).
[28]D. Han, M. E. Noz, Y. S. Kim, and D. Son, Phys. Rev. D **27**, 3032 (1983).
[29]This commutator can be translated into wave-function formalism. For a wave-function description of this commutation relation, see M. J. Ruiz, Phys. Rev. D **10**, 4306 (1974).
[30]For a pedagogical treatment of the light-cone coordinate system, see Y. S. Kim and M. E. Noz, Am. J. Phys. **50**, 721 (1982).
[31]Y. S. Kim and M. E. Noz, Found Phys. **9**, 375 (1979); J. Math Phys. **22**, 2289 (1981).
[32]R. P. Feynman, in *High Energy Collisions*, Proceedings of the Third International Conference, Stony Brook, NY, edited by C. N. Yang *et al.* (Gordon and Breach, New York, 1969); *Photon Hadron Interactions* (Benjamin, New York, 1972). See also J. D. Bjorken and E. A. Paschos, Phys. Rev. **185**, 1975 (1969).
[33]P. E. Hussar, Phys. Rev. D **23**, 2781 (1981).

Understanding some simple phenomena in thermoacoustics with applications to acoustical heat engines

John Wheatley, T. Hofler, G. W. Swift, and A. Migliori
Condensed Matter and Thermal Physics Group, MS K764, Los Alamos National Laboratory, Los Alamos, New Mexico 87545

(Received 29 November 1983; accepted for publication 15 March 1984)

Thermoacoustical phenomena have a long history and are frequently characterized by great complexity. In the present paper, we describe how, by the use of suitable acoustical structures, the phenomena can both be simplified and readily demonstrated. A heuristic discussion is emphasized, which we hope will be useful in teaching the principles. The qualities of certain model apparatus that demonstrate acoustically stimulated entropy flow, a thermally driven acoustic oscillator, and an acoustically driven refrigerator are also presented in semiquantitative detail.

I. INTRODUCTION

Thermoacoustical phenomena have been studied seriously for over two centuries. A review of Putnam and Dennis[1] describes experiments of Byron Higgins[2] in 1777 in which he was able to excite organ pipe oscillations in a large tube, open at both ends, by suitable placement of a hydrogen flame inside. Perhaps the best known thermoacoustical devices are the Sondhauss tube,[3] described in 1850, and the Rijke tube,[4] described in 1859. In some historical remarks Rott[5] notes that Sondhauss had referred to some earlier work in 1804, while the Rijke tube itself is, in some sense,

© 1985 American Association of Physics Teachers

This article is copyrighted as indicated in the article. Reuse of AAPT content is subject to the terms at: http://scitation.aip.org/termsconditions. Downloaded to IP: 95.68.109.7 On: Wed, 23 Apr 2014 04:24:23

an extension of Higgins' work. Physicists today often encounter the thermoacoustic "Taconis" oscillations[6] when a tube is inserted into a cryogenic storage vessel. These oscillations have been studied recently experimentally in some quantitative experiments by Yazaki *et al.*[7] Of the different types of heat-operated acoustic oscillators described above, the Sondhauss oscillator and configuration is the closest to those which are the subject of this paper. These have been reviewed relatively recently by Feldman,[8] who makes the important point that the oscillations can be modified by the placement of suitable structures within the resonating tube.

Imposed fluctuating gas pressures in a tube can also, for suitable conditions and configurations, lead to the production of cold. Gifford and Longsworth[9] demonstrated this for very low-frequency, very large pressure variations in an internally structure-free cylinder with one end closed and the other connected to a regenerator. They called this device a "pulse-tube." A cooling was also observed by Merkli and Thomann[10] near the *velocity* antinode of gas resonating in a tube closed at one end with a plug and at the other end with an oscillating piston.

A theoretical understanding of these various phenomena goes back to Lord Rayleigh[11] whose discussion, though largely qualitative in nature, emphasizes the importance of the time phase between temperature and motion. This point goes to the heart of the matter. Modern quantitative understanding of the phenomena most relevant to the present work is to be credited to Rott and co-workers[5,12–18] whose notation we use wherever practical in this article.

Our initial approach[19–22] to the subject of thermoacoustics was more from the standpoint of thermodynamics than that of acoustics. We considered the acoustical context primarily as a means for demonstrating some very general principles governing what we call "intrinsically irreversible heat engines" or, alternatively, "natural engines." In such engines, the all-important concept of the phase between thermodynamic effect (e.g., temperature) and motion, first emphasized by Lord Rayleigh, is introduced into the engine by means of some natural irreversible process, such as thermal conduction. Examining the thermoacoustical phenomena from the point of view of heat engines has proven to be particularly fruitful.

The paper is organized along the following lines. We begin by showing *what* happens experimentally in several simple thermoacoustic devices. First, we describe an extremely simple acoustical system containing what we call a "thermoacoustic couple,"[21,22] constructed using cheap and commonly available materals so that it can readily be adapted to senior-level laboratories. This device demonstrates one of the basic thermoacoustic effects, an acoustically stimulated hydrodynamic entropy flow, by introducing a second thermodynamic medium, a small stack of plates, into the basic acoustical structure. Then we describe two more devices and how they perform. One is a thermally driven oscillator (a prime mover). In the second, heat is transferred from one place to another as a consequence of applied acoustical power (a heat pump or refrigerator). With both the apparatus and some experimental observations now laid out with some completeness, we digress briefly to review some thermodynamical and acoustical concepts as well as to introduce notation. Then we proceed heuristically in a context of a general fluid having vanishing viscosity (or zero Prandtl number) to describe concepts such as heat flow, work flow, critical temperature gradients, and efficiency (or coefficient of performance). Actual formulas for nonzero Prandtl numbers will be quoted and compared with those derived heuristically if the comparisons are relatively transparent. We present both the model thermally driven oscillator and the model acoustically driven refrigerator in sufficient detail to allow others to reproduce them, if desired. Additionally, we describe some simple quantitative measurements on the models which give further insight into how they actually work. The article is completed with some general remarks on natural engines of which thermoacoustic engines are an important example.

II. THE THERMOACOUSTIC COUPLE (TAC)

Apparatus for demonstrating easily a fundamental thermoacoustic effect can be built very easily and inexpensively as shown schematically in Fig. 1. Most components were obtained from nearby hardware and chemical supply stores. The driver is an inexpensive full-range speaker obtained from a local electronics supply store. The thermocouple wires needed to detect the TAC output may be more difficult to find locally. They are 0.003-in. diam Chromel and Constantan wires with Teflon insulation. Five such thermocouples in series produce a thermal EMF of about 298 μV per C° temperature difference.

The apparatus of Fig. 1(a) is nothing more than a simple driven acoustical resonator constructed so that it can be easily assembled and disassembled and with the possibility of readily inserting a small stack of plates, the thermoacoustic couple, at a controlled and measurable position inside the resonant tube. The stack of plates itself is closely related to Rev. Robert Stirling's invention of 1816,[24] which we have called[25] introduction of a "second thermodynamic medium" (the gas is the primary or first thermodynamic medium) with one crucial exception. Stirling's second medium had the function of rendering all processes with the primary medium locally isothermal, this result being achieved by adjusting the geometry, the frequency, and the heat capacity of the second medium so that gas near a given location in the second medium always had the temperature of that location. In the present case, the second medium is also essential and still should have a high effective heat capacity compared with the effective heat capacity of the adjacent fluid. But in the present engines the second medium acts as a thermal lag in establishing a suitable phase relationship between temperature and motion in the primary fluid. It is also usually desirable that over a substantial fraction of the primary fluid the acoustical processes be essentially adiabatic. (We note in passing that the thermoacoustic traveling wave engine suggested by Ceperley[26] is, as he points out, a true Stirling engine rather than a type of natural engine similar to the ones we are describing here.)

The apparatus of Fig. 1(a) is inadequately instrumented to do really quantitative work, not to mention the difficulties in interpretation that arise from the imperfect geometry. To do semiquantitative work, we first replaced the cork and TAC structure with a dynamic pressure transducer, which gave roughly the same free volume at the end and which had been calibrated absolutely in other experiments.[27] With this configuration we then chose the resonant frequency to be used in the later thermal measurements and plotted dynamic pressure *amplitude* P_0 versus driver current, as in the actual experiments the pressure transducer is removed and only the driver current could be measured. Such a procedure was adequate for present pur-

This article is copyrighted as indicated in the article. Reuse of AAPT content is subject to the terms at: http://scitation.aip.org/termsconditions. Downloaded to IP: 95.68.109.7 On: Wed, 23 Apr 2014 04:24:23

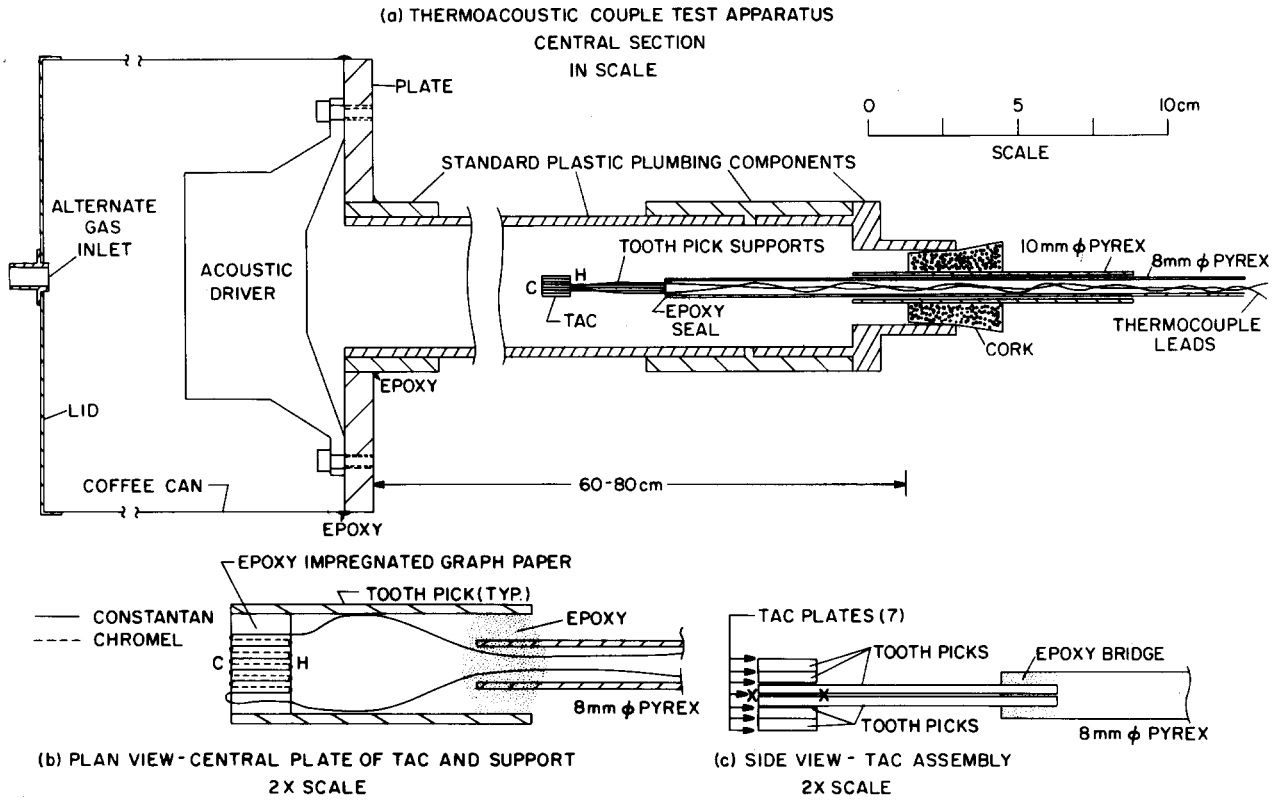

Fig. 1. Scale drawing of a simple thermoacoustic couple test apparatus shown in enough detail to permit construction by senior laboratory students. (a) A central section indicating construction and placement of parts. No glue is needed on any of the plastic parts except as noted; this allows easy disassembly and change. A possible acoustic driver is listed in Ref. 23. (In the USA, the plastic pipe and associated fittings have a nominal 1 $\frac{1}{8}$-in. i.d.) The 8-mm-diam Pyrex tube is selected so that it just slides within the 10-mm-diam Pyrex tube as excessive leakage is undesirable. The lid of the coffee can is fitted with a small nipple that can either be corked or used to admit gases other than air using a continuous flow-through method. Acoustic resonance tubes can be changed as desired to alter the overall length of apparatus. Electrical leads for the driver can be extracted using epoxy-sealed leads in the front plate. (b) Shows in double scale how the five-couple Chromel–Constantan thermopile is assembled via epoxy onto the central plate of 0.0165-cm-thick epoxy-impregnated graph paper, and then, using suitable jigs and fixtures, sealed via its 1-mm-thick toothpick supports, to the 8-mm-diam Pyrex tube which serves both to extract the thermopile leads and to allow free positioning of the TAC within the acoustically resonant tube. (c) Shows a side view of the TAC assembly indicating how the three guard plates on each side, also made of epoxy-impregnated graph paper, are spaced from the central plate by additional epoxied 1-mm-thick toothpicks. The TAC support toothpicks are fixed to the 8-mm-diam tube and the leads sealed by a judicious use of paper and more epoxy. Each ($\times$) represents a line of five Chromel–Constantan joints.

poses. An example of the thermocouple EMF vs TAC position in air at a mean pressure p_m of 0.787 bar, the local atmospheric pressure, a resonant frequency of 458.5 Hz, and ambient temperature of 22.7°C, and a dynamic/static pressure ratio of $P_0/p_m \simeq 3.6\times 10^{-3}$ is shown in Fig. 2. Here negative values of thermocouple EMF E correspond to C being colder than H on Fig. 1(a). The support structure of the TAC prevents measurements near the pressure antinode at the closed end but the pattern is clear (see also Refs. 21 and 22). There is essentially a sinusoidal dependence of temperature difference on position with zeros at both pressure and velocity nodes (or antinodes) and with the hot end of the TAC closest to the nearest pressure antinode.

As the relative drive P_0/p_m increases, the data corresponding to those in Fig. 2 change from the nearly perfect sinusoid shown there to something closer to a sawtooth shape, with the maxima (minima) shifted to be near the pressure antinodes. There are still zeros at velocity and pressure antinodes, but the slope of the curve is very steep and negative at the pressure antinodes.

Although we will give a more detailed explanation of these phenomena later, it is helpful to note now that what is happening here is an acoustically stimulated convective or hydrodynamic entropy flow in the gas within the thermal skin depth [see context of Eq. (10)], the entropy departing the plates and, hence, cooling them at one end while entering the plates and hence heating them at the other. As the plates of the TAC are more or less thermally isolated from the walls, the whole process is in steady state when the hydrodynamically flowing entropy in the gas is just balanced by a return diffusive entropy flow in the material of the plates and in the surrounding gas. The so-called guard plates act to increase the ratio of the diffusive conduction in the plates to that in the gas, the effect being to increase the temperature difference developed by the TAC at a given acoustic power level. Naturally, a work flow is necessary to produce the entropy flow, and for short plates this work flow will turn out to be roughly proportional to the length of the plates.

The hydrodynamic entropy flow in the gas mentioned above is greatest when there is no average temperature gradient in the plates of the TAC. As the acoustically stimulated temperature gradient develops the entropy flow diminishes. There is a concept of a critical temperature gradient, beyond which acoustical power alone cannot increase the

This article is copyrighted as indicated in the article. Reuse of AAPT content is subject to the terms at: http://scitation.aip.org/termsconditions. Downloaded to IP: 95.68.109.7 On: Wed, 23 Apr 2014 04:24:23

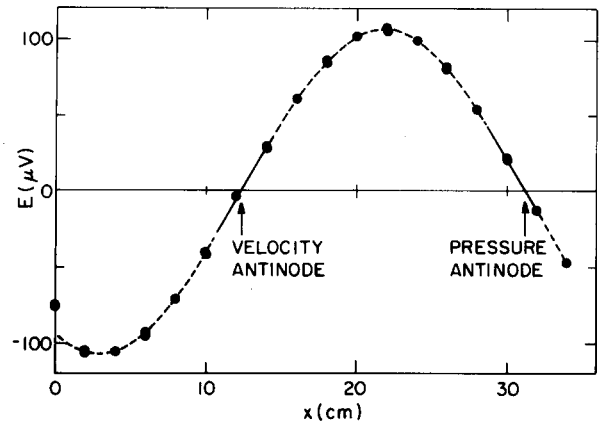

Fig. 2. Dependence of EMF E of electrical thermopile on the axial position x (arbitrary zero) of the thermoacoustic couple (TAC) along the resonance tube of Fig. 1. Increasing values of x correspond to movement of the TAC away from the closed end of the resonant tube. The line through the points is a perfect sinusoid fitted to the zero crossings and to the average of the absolute values of the extrema. The locations of the velocity and pressure antinodes as determined by the TAC are shown on the figure. The gas is air at a mean pressure $p_m = 0.787$ bar and temperature 22.7°C. The TAC is the same one illustrated schematically in Fig. 1 and shown photographically in Fig. 13(a). Resonance frequency is 458.5 Hz. The ratio of the peak dynamic pressure P_0 to the mean pressure is $P_0/p_m = 3.6\times10^{-3}$.

temperature gradient along the plates, even in the absence of effects such as longitudinal diffusive thermal conduction or gas viscosity. In the region of temperature gradients from zero to critical, heat pumping action occurs. If, now, external sources of heat are applied to the ends of the plates, which cause the temperature gradient to sufficiently exceed the critical gradient, the acoustic system may spontaneously oscillate and we have what might be called a prime mover.

III. SOME MODELS OF ACOUSTIC ENGINES

An example of a prime mover, a thermally driven oscillator, is shown in scale in Fig. 3. For the device to oscillate, the closed end must be hotter than the open end. As much of our work is cryogenic in nature, this device was designed to operate with the closed end kept warm by the hands and the open end cooled as needed by liquid nitrogen. The "engine" is made using two brass flanges separated by a short length of poorly thermally conducting stainless steel tube and filled with 22 G-10 fiberglass plates, each 0.38 mm wide and spaced from one another by 1.00 mm. The lengths of the plates were cut to conform to the inner diameter of the stainless steel tube. All the fiberglass plates had a common height of 16.5 mm. The ends of the fiberglass plates were epoxied to copper strips, also 0.38 mm wide by 1.6 mm high. These copper strips were extra long so that, spaced by additional copper pieces at the flanges, they could be secured with low-melting-point solder to the brass flanges. In construction, one copper strip was first epoxied to each fiberglass plate, but application of the second copper strip and epoxying and soldering of all parts together, holding the correct interplate spacing, was more complex. For demonstration, the open copper tube was 35 mm o.d. × 32.4 mm i.d. × 144 mm long; the closed tube had the

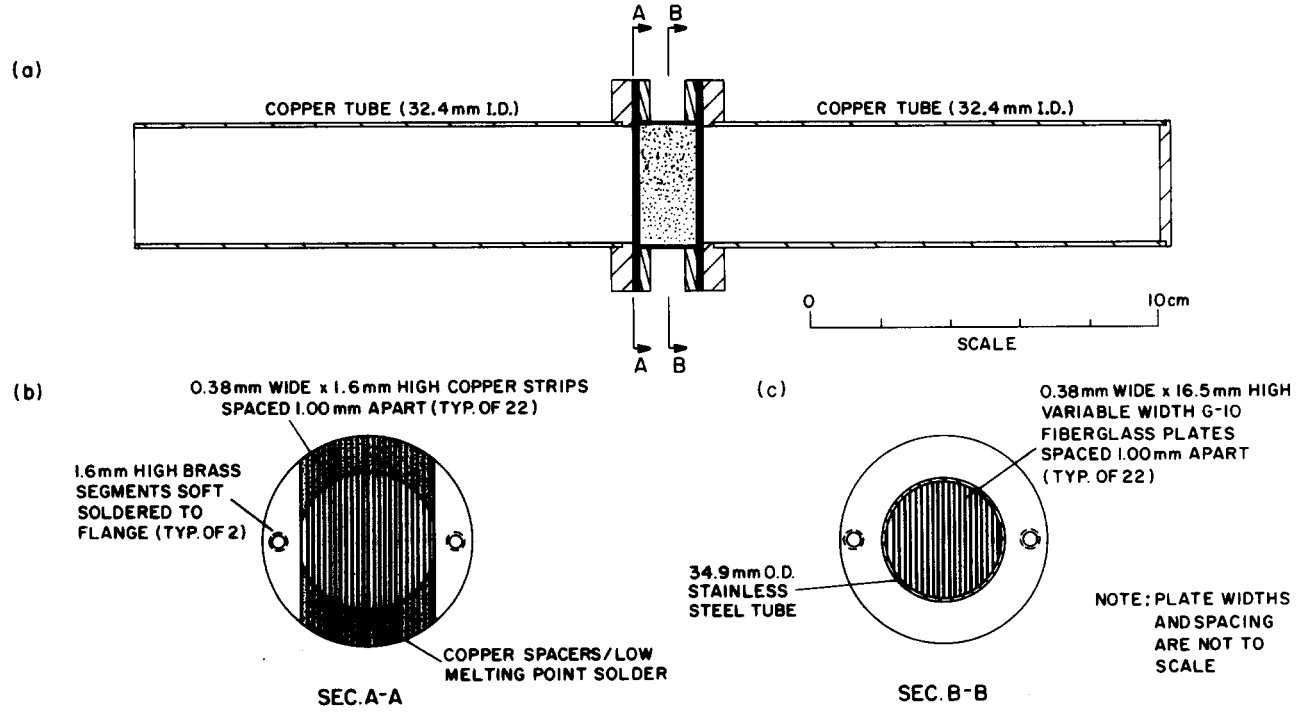

Fig. 3. Scale drawing of a simple thermoacoustic oscillator which operates between room temperature and a cold temperature in excess of liquid N_2 temperature. (a) A central section through the oscillator indicating the three demountable parts: an open copper tube and a closed copper tube connected by flanges to a central short "engine section" consisting of 0.38-mm-wide × 16.5-mm-high variable length G-10 fiberglass plates packed with a uniform 1.00-mm plate-to-plate spacing in a 34.9-mm-o.d. thin wall stainless steel tube and making mechanical contact to 0.38-mm-wide × 1.6-mm-high copper thermal contact strips using Stycast 2850 FT epoxy. The copper thermal contact strips in the region of the engine flanges are spaced by ca. 1-mm-wide copper pieces and adhered using a low-melting point solder. (b) Shows Sec. A–A giving an end view of the engine section while (c) shows Sec. B–B which indicates how the G–10 fiberglass plates are packed uniformly and with a close fit to the walls of the stainless-steel tube. The purpose of the stainless steel is to act as a thermal insulator.

This article is copyrighted as indicated in the article. Reuse of AAPT content is subject to the terms at: http://scitation.aip.org/termsconditions. Downloaded to IP: 95.68.109.7 On: Wed, 23 Apr 2014 04:24:23

same o.d. and i.d. and was 131 mm long inside. The "engine" assembly, including flanges that were "sealed" to the copper tubes by a "heat sink" compound, was 20 mm long. In operation, the cold end is immersed in liquid nitrogen with liquid level near the engine flange while the other end is kept warm with one's hands. When the open end is adequately cold, one can actually feel the whole tube shake at a very low frequency, corresponding to oscillations of the gas column and the liquid nitrogen. The tube is now withdrawn from the liquid nitrogen and will "sing" loudly and longly at a frequency of ca. 200 Hz, which increases as the tube warms. In a modification of this procedure, once the tube is singing one can use a jet of helium gas temporarily directed into the tube to replace the air, with a dramatic increase in both frequency and intensity of the emitted sound. We call this device the "Hofler" tube, after one of the co-authors, as it was designed and built by him to demonstrate some thermoacoustic phenomena to his doctoral committee.

By replacing the closed end of the tube of Fig. 3 with a part of similar diameter, length, and volume but with a calibrated[27] dynamic pressure transducer; and furthermore, by attaching a differential thermocouple of Chromel–Constantan to the copper strips at opposite ends of a centrally located fiberglass plate, it is possible to make a number of interesting quantitative measurements on this simple device, some of which will be detailed near the end of the paper. In order to control the temperature conditions more effectively, we attached a heavy copper plate at right angles to the "cold" side of the "engine" flange and crudely thermally insulated the open copper tube. This transverse external copper plate could be immersed in liquid N_2 to various levels in order to adjust the temperature level of the open tube while a heating tape provided heat as required to keep the closed copper tube at a relatively constant temperature near ambient. We show in Fig. 4 some examples, taken at different thermal drives, of the buildup of pressure oscillations in air at the closed end of the tube once the temperature ratio across the engine has become large enough. These photographs were taken by capping the open end of the tube loosely with an insulating plate and then suddenly removing the plate. The zero of time is determined by the triggering level on the oscilloscope and hence has no significance. In Fig. 4(a) we catch the oscillations at a relatively early stage of their development when the pressure amplitude is increasing rather accurately exponentially in time. In Fig. 4(b) both the initial exponential rise and the development of a steady state can be seen, the latter peak-to-peak pressure variation exceeding 11% of the ambient pressure.

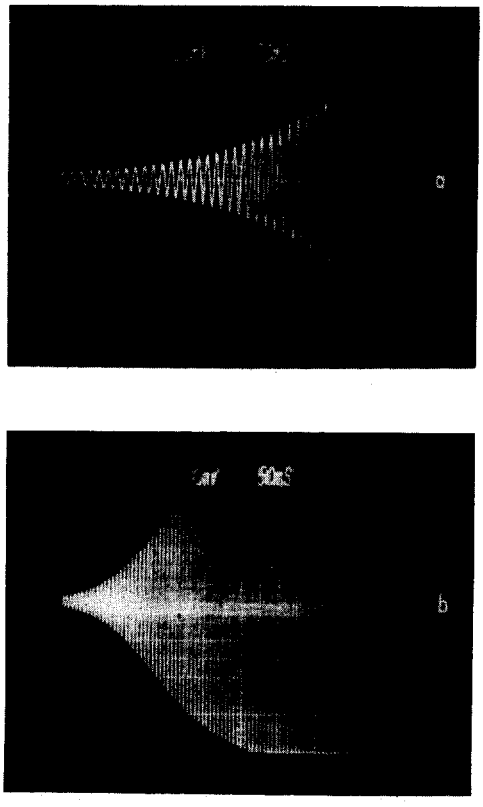

Fig. 4. Time development of the oscillations in pressure at the closed end of the heat-driven oscillator of Fig. 3. The pressure calibration is approximately 0.054 bar per volt, with a mean pressure of 0.78 bar. (a) A signal in the early stages of development. Fifty mV per main vertical division; 20 ms per main horizontal division. (b) A signal in a developing state which then saturates. Two hundred mV per main vertical division; 50 ms per main horizontal division. The peak-to-peak maximum dynamic pressure oscillation is 11% of the ambient pressure for this case.

An example of an acoustic refrigerator is shown in Fig. 5. We regard this apparatus as a major improvement on equipment used for a similar purpose in previous work by us.[19,22] Figure 5 shows a much more complex device than the model thermoacoustic oscillator of Fig. 3 owing not only to the need for an acoustic driver but also to the requirements for a low heat input to the "cold" end and excellent heat removal at the "hot" end if substantially low temperatures are to be achieved. As the construction is complicated we reserve discussion of many of the details to the Appendix. The parts are simple conceptually. Referring to Fig. 5, there is an acoustic driver D in a pressure vessel so that in the experiments ^{4}He gas at ca. 10 bar means pressure can be used as primary working fluid. In a refrigerator it is desirable to drive the system from the top with a pressure antinode there, so the acoustic impedance is high near the driver. A special piston and "surround," labeled P, are attached to the driver to match it to such a high impedance. Dynamic pressure measurements were made using a small microphone at M. A very small capillary, not shown, allowed the average pressure to equalize across P but with a long relaxation time compared to the acoustic period. The second medium S had a longitudinal length of 82.4 mm and consisted of a roll of 0.076-mm-thick Kapton film with open spaces between wraps of ca. 0.38 mm wound uniformly on a 6.4-mm-diam cloth phenolic rod out to a diameter of 38.1 mm. It fit tightly in a fiberglass tube and was supported at the bottom end C by a cross made of thin stainless steel sheets. The upper heat exchanger H consisted of a stack of four copper screens soldered along their periphery to an insert which made contact with the rest of the upper assembly using Dow Corning 340 silicone heat sink compound. We regard this heat exhange system as inadequate, but suitable for the demonstration required for this paper. Below the second medium, the resonant tube necks down to a 22-mm-i.d. copper tube T which terminates in a 100-mm-i.d. can V of ca. 1 liter volume to complete the acoustically resonant system. An alternative resonator might have used a uniform diameter tube below S adjusted for half-wave resonance. But a detailed analysis, to be published elsewhere, showed that the overall acoustic losses below C, which, in an insulated system, must eventually appear as

This article is copyrighted as indicated in the article. Reuse of AAPT content is subject to the terms at: http://scitation.aip.org/termsconditions. Downloaded to IP: 95.68.109.7 On: Wed, 23 Apr 2014 04:24:23

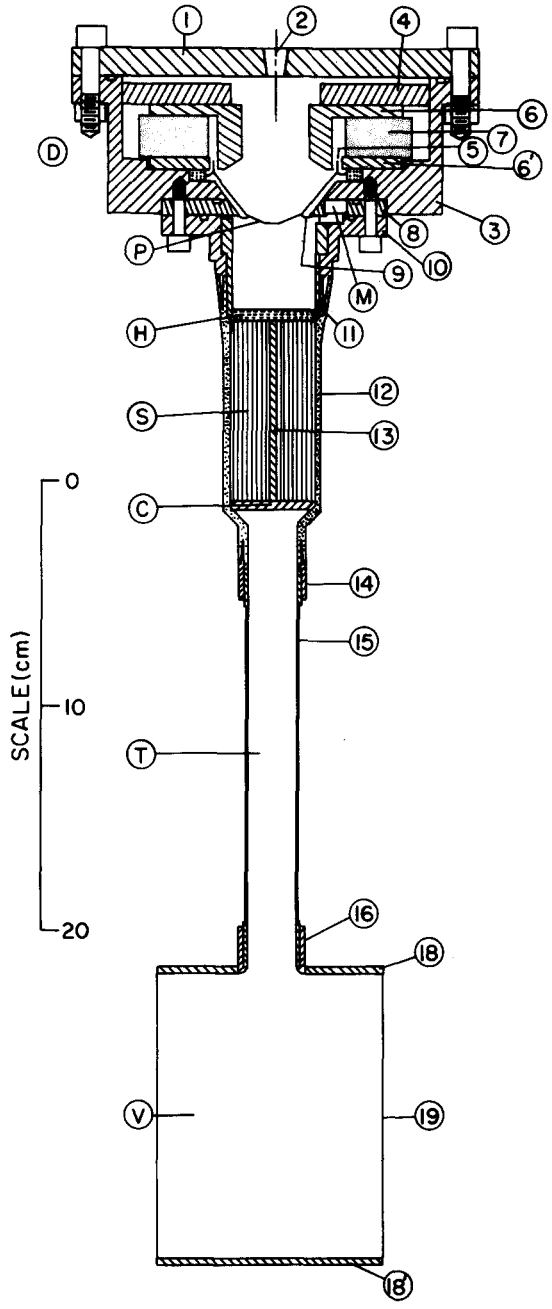

Fig. 5. Acoustically driven cooling engine drawn to scale. The lettered components are the principal parts. Numbered components and other details of the construction are referred to in the Appendix. The acoustic driver and pressure assembly is D. P is a thin aluminum part with associated "surround" which acts as an oscillating piston to drive the helium working gas in resonance with a pressure antinode near P. M is the location of the microphone used to sense dynamic pressure. H is the "hot" heat exchanger. S is a second thermodynamic medium consisting of a roll of Kapton film with a uniform spacing. C is the cold end of the second medium and a "cross" of thin stainless-steel sheets used to support S. T is a smaller diameter tube and V a 1-liter volume gas spring which together comprise that part of the resonant acoustic system below S.

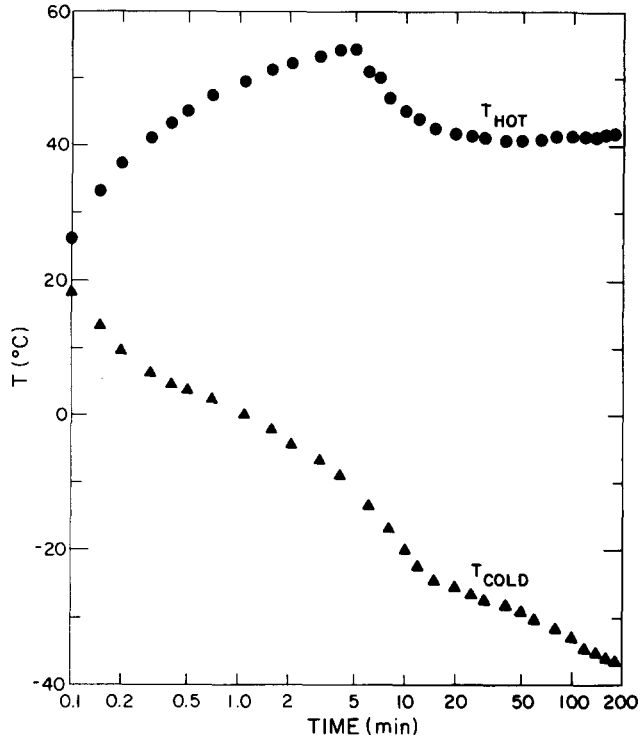

Fig. 6. An example of the change of temperature with time (plotted on a logarithmic scale) for the acoustic cooling engine shown in Fig. 5. All parts below the driver have been thermally insulated with about 15 wraps of super-insulation and arranged to be in a vacuum with a pressure of about 1μ of mercury. Thermocouples placed inside the engine at the hot heat exchanger and at the cold end of the second medium (locations H and C on Fig. 5) indicated the temperatures $T_{\rm Hot}$ (●) and $T_{\rm cold}$ (▲) shown on the graph for those regions of the engine. The nonmonotonic variation of T_H with time is ascribed both to a temperature dependent behavior of the Dow Corning 340 heat sink compound used to facilitate thermal contact between the heat sink and the rest of the driver and to the application several minutes into the run of cooling water in coils located outside the driver's pressure vessel. In these measurements, the mean pressure p_m is 10.3 bar, the dynamic pressure amplitude P_0 is 0.034 of p_m or 0.35 bar, and the frequency is 516 Hz. In spite of the fact that this device is the first of a kind, has a number of technical defects, and is not optimized, a substantial temperature difference has been achieved across the second medium. The heat load at C is of order 0.6–0.8 W.

heat at C, are substantially less with the necked-down tube T and the gas spring V than with a uniform tube.

A test run with the apparatus of Fig. 5, with the parts below D insulated with ca. 15 wraps of superinsulation and immersed in a vacuum of 10^{-3} Torr, is shown in Fig. 6. The temperature at H, $T_{\rm HOT}$, and that at C, $T_{\rm COLD}$, are shown as a function of time, plotted logarithmically, following turning on the acoustic power. (The initial temperatures of H and C were not exactly the same.) For these observations, the mean pressure was 10.3 bar ^{4}He. Near the end of the test the amplitude P_0 of the dynamic pressure measured at M was 0.034 of the mean pressure, or 0.35 bar, and the frequency was 516 Hz. Even after 200 min into the test, a thermocouple on the outside of V still indicated -17°C and cooling. At this time the refrigeration at C is estimated to be of order 0.6–0.8 W. We believe that the nonmonotonic behavior of $T_{\rm HOT}$ with time can be attributed both to changes in thermal contact with the driver assembly caused by changes in the heat sink compound's effective thermal conductance and to the initiation of water cooling of the outside of the pressure vessel some minutes after the test began. Although the model in Fig. 5 is the first form of an acoustic cooling apparatus intended eventually for quantitative measurements, the results in Fig. 6 clearly show that substantial cooling can be achieved with it by acoustic means. A number of improvements to the model of Fig. 5 are underway, and we expect substantial improve-

This article is copyrighted as indicated in the article. Reuse of AAPT content is subject to the terms at: http://scitation.aip.org/termsconditions. Downloaded to IP: 95.68.109.7 On: Wed, 23 Apr 2014 04:24:23

ments even over the results in Fig. 6. A detailed discussion of the design and operation of acoustic refrigerators will be presented in a later publication.

IV. A BRIEF REVIEW OF PRINCIPLES AND NOTATION

Most notation where possible is the same as that used by Rott.[5] In the fluid, the first-order fluid displacement and velocity parallel to the axis of the tube in which the resonating fluid is contained will be called, respectively, x_1 and u_1. The dynamic pressure p_1 is assumed to depend only on the position x along the axis of the tube and not on the lateral position. The dynamic termperature T_1 will be assumed to be essentially zero at the walls, corresponding to the walls having a much higher effective heat capacity per unit area than the fluid. Far from the walls the dynamic fluid temperature will take on its adiabatic value $T_{1_{ad}}$. Mean quantities, where confusion may arise, will be given a subscript m, as mean pressure p_m, mean density ρ_m, mean temperature T_m. The sound velocity a is related to the adiabatic compressibility k_s by the equation

$$\rho_m a^2 = k_s^{-1}, \tag{1}$$

where, using the standard thermodynamic definition, s being entropy, we have

$$k_s = \frac{1}{\rho}\left(\frac{\partial \rho}{\partial p}\right)_s. \tag{2}$$

The acoustic impedance is defined to be $\rho_m a$. In a plane wave lossless cylindrical acoustic resonator, the dynamic pressure amplitude P_0 at a *pressure* antinode is related to the amplitude of the velocity U_0 at a velocity antinode by the equation

$$P_0 = (\rho_m a) U_0. \tag{3}$$

There are one or two important formulas from elementary thermodynamics which we require. Assuming that (p_1/p_m) and (T_1/T_m) are both very small compared to unity, then the adiabatic temperature change caused by a pressure change p_1 is

$$T_{1_{ad}} = (T_m \beta / \rho_m c_p) p_1, \tag{4}$$

where β is the isobaric expansion coefficient,

$$\beta \equiv -\frac{1}{\rho_m}\left(\frac{\partial \rho_m}{\partial T_m}\right)_{p_m}. \tag{5}$$

The specific heat at constant pressure per unit mass is c_p, so that $\rho_m c_p$ is the specific heat at constant pressure per unit volume of fluid. We shall see that $T_m \beta$ (which is unity for the ideal gas) can be called the "heat parameter" of a fluid.

Work in engines of the present type depends on the difference $k_T - k_s$ between the isothermal and adiabatic compressibilities of the fluid. It can be written

$$k_T - k_s = \beta (T_m \beta / \rho_m c_p) = (\gamma - 1) k_s, \tag{6}$$

where γ is the ratio c_p/c_v of the specific heats at constant pressure and at constant volume while k_s can be found from (1) or (2). The quantity $(\gamma - 1)$ can be called the "work parameter" of the fluid.

Important quantities also for the present engines are the irreversible processes of the diffusion of heat and of momentum (or vorticity). In a simple harmonic wave of angular frequency ω the scale of distances within the fluid over which the walls affect the fluid as a result of these irreversible processes is determined by the simple law of diffusion, which for one-dimensional diffusion in the y direction, is given by the well-known equation

$$\langle y^2 \rangle^{1/2} = (2Dt)^{1/2}. \tag{7}$$

This equation describes the rms displacement $\langle y^2 \rangle^{1/2}$ of particles at time t in a medium for which the particles have diffusion coefficient D and into which they are released at $t = 0$, $y = 0$. The distance scales for the diffusion of temperature (or heat), for which $\langle y^2 \rangle^{1/2}$ is replaced by the thermal penetration depth δ_κ, and vorticity, for which $\langle y^2 \rangle^{1/2}$ is replaced by the viscous penetration depth δ_ν are obtained by substituting into (7), for t the quantity ω^{-1}, and for D either the thermal diffusivity (or thermal diffusion coefficient)

$$\kappa \equiv K / \rho_m c_p, \tag{8}$$

or the kinematic viscosity (or viscous diffusion coefficient)

$$\nu \equiv \eta / \rho. \tag{9}$$

These then give the results

$$\delta_\kappa = (2\kappa/\omega)^{1/2} \tag{10}$$

and

$$\delta_\nu = (2\nu/\omega)^{1/2}. \tag{11}$$

In the above, K is the thermal conductivity and η is the dynamic viscosity. Both κ and ν have, for example, dimensions of cm^2/s, just as for D.

The ratio

$$\sigma \equiv \nu / \kappa \tag{12}$$

is called the Prandtl number. It plays a very important role in acoustic engines, describing the relative diffusion coefficients for vorticity and heat. For most gases near room temperature, e.g., helium or air, we have $\sigma \simeq 2/3$. But for liquid metals like Na at practical temperatures, we have $\sigma \simeq 0.004$, so that in liquid metals viscous effects are quite small compared with those of thermal conduction.

V. SOME HEURISTIC DESCRIPTIONS OF THERMOACOUSTICAL PHENOMENA

A. Understanding the existence of entropy flows in the thermoacoustic couple

We can still have a reasonably accurate picture of what is happening in the TAC and the preceding heat pumping and prime moving engines if we use the limit of zero Prandtl number σ, so that the viscous penetration depth δ_ν is negligible and the fluid flows like a plug, slipping along the boundary. Some of the arguments presented below were originally worked out in a context of "pulse tubes" by Gifford and Longsworth,[9] and we have simply adapted them to our acoustic examples.

The behavior of the TAC can be understood qualitatively by imagining a single short plate, shown sectioned in Fig. 7, inserted into the end of an acoustic resonator. The plate is short compared both with its distance from the closed end and the radian length λ of the acoustic wave and long compared with the acoustic displacement amplitude. The plate has a high effective heat capacity per unit area and *uniform temperature throughout*. We are going to imagine what happens thermally to three parcels of fluid, (a), (b), and (c). These are located at least part of the time within a thermal penetration depth δ_κ from the plate and, as a consequence of the pressure fluctuations, reciprocate between,

This article is copyrighted as indicated in the article. Reuse of AAPT content is subject to the terms at: http://scitation.aip.org/termsconditions. Downloaded to IP: 95.68.109.7 On: Wed, 23 Apr 2014 04:24:23

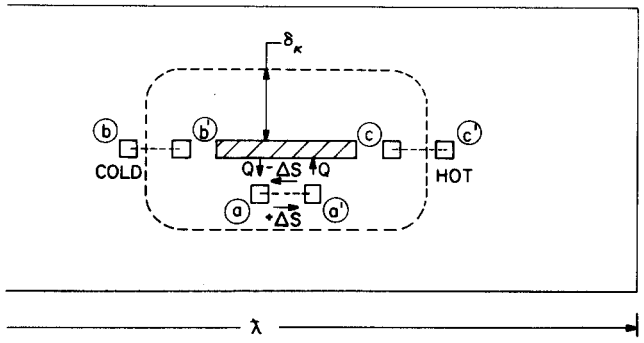

Fig. 7. Schematic diagram illustrating the acoustical stimulation of hydrodynamic entropy flow in a zero Prandtl number fluid near a plate (cross hatched) inserted near the closed end of an acoustically resonant tube. (a), (b), and (c) are three parcels of fluid located, respectively, near the center and at opposite ends of the plate and moving between (a) and (a'), (b) and (b'), and (c) and (c'). At least part of the time each parcel is "on speaking terms" thermally with the plate. The dashed line around the plate represents the extent of the thermal penetration depth δ_κ. The plate has a high effective heat capacity per unit area and a *uniform* temperature throughout, in particular no temperature gradient along the direction of the reciprocating fluid motion. In the text it is assumed that the plate length is short compared to its mean distance from the closed end of the resonant tube and that both are small compared to λ in order to simplify the discussion. The heat flows Q and entropy increments ΔS are described in the text.

respectively, (a) and (a'), (b) and (b'), and (c) and (c'). To simplify thinking further, imagine that the sinusoidal cycle accompanied by thermal lag is replaced by an articulated cycle: rapid motion–wait–rapid motion–wait–etc. Consider first parcel (a). As it moves rapidly from (a) to (a'), there is no time for heat flow, so that its entropy remains constant. But at (a'), as it has been pushed by the fluid behind it, the pressure is increased and the temperature increased by the adiabatic amount, Eq. (4). As the fluid at (a') is now hotter than the plate and close enough to the plate for heat to transfer to it, heat Q passes from the parcel to the plate, thereby *decreasing* the entropy of the parcel by some amount ΔS. The rapid motion from (a') to (a) is again adiabatic, so the entropy carried to the left is diminished by ΔS. The gas pressure is reduced at (a), so the temperature is now reduced below that of the plate by the adiabatic amount. Hence, heat Q flows into the parcel from the plate, thereby *increasing* the entropy of the parcel by ΔS. In the subsequent adiabatic motion from (a) to (a'), this entropy increment is unchanged. Hence, in one complete cycle entropy $2\Delta S$ has been carried from left to right. The same conclusion holds for all parcels which, like (a), are in contact with the plate at each end of the stroke. Excepting near the ends, if one parcel adds heat Q to one piece of the plate during one part of a cycle, another parcel will remove that same amount of heat from the same piece during another part of the cycle (for a short enough plate, but that is a detail); the average thermal condition of the plate remains unchanged while entropy flows on the average hydrodynamically along the plate in the fluid, within a lateral distance of order δ_κ from the plate, toward the pressure antinode. But at the ends, where the symmetry of the heat transfer is broken, the physics is a little different. Consider the parcel (b) which in its trajectory moves in and out of thermal contact with the plate. In the compressed state at (b') it is in contact with the left end of the plate, but when it expands and moves to (b) it loses thermal contact and simply remains cold. On compression from (b) to (b') there is an adiabatic temperature increase, but in steady state this just increases the temperature back up to the temperature of the left end of the plate. Hence, the fluid to the left of the left end of the plate will have a lower temperature than the adjacent plate by the fluid's adiabatic temperature difference. Moreover, parcel (b) plays no average role in the average heat flow while parcels like (a) but near the left end of the plate have an uncompensated heat extraction effect. As a consequence there is a net diffusive heat extraction rate from the left end of the plate. Note that while $T_{1_{ad}}$ may be small, so is δ_κ; so the temperature gradient for this diffusive heat transfer there can be substantial. Similarly, consider the parcel (c) which in its trajectory also moves in and out of thermal contact with the right end of the plate. The motion (c)↔(c') is essentially adiabatic. Fluid at (c) has the same temperature as the right end of the plate while, when the fluid is at (c') there is no thermal contact. As (c') is the compressed state, the fluid to the right of the right end of the plate is hotter then that end of the plate by the adiabatic temperature difference. Again, parcel (c) plays no role in the heat transfer at the right end, so parcels like (a') but at the right end have uncompensated heat flows into the right- hand end of the plate. If the plate is made of a highly thermally conducting material, e.g. copper, very little temperature difference will occur across the plate, but the entropy flow will be maximum. In that case, on the average, entropy flows diffusively out of the cold end of the plate into the fluid, hydrodynamically in the fluid in the thermal skin depth adjacent to the plate towards the hot end and then back into the plate at the hot end. The same entropy flows diffusively within the conducting plate from hot to cold, completing the circuit. (For a short enough plate, the entropy circulated per cycle is much larger than that generated per cycle, which we have in fact neglected.)

B. Understanding heat pumping engines, critical temperature gradients, and prime moving engines

The physics of the devices to be discussed here is very similar to that of the TAC but with a few notable exceptions. The ideal TAC measures entropy flow and from that a quantity proportional to the product of acoustical pressure and velocity. The longitudinal thermal conductance is generally made large enough to assure that substantial temperature gradients, which can modify the entropy flow, do not occur. And furthermore, the length of the couple is kept short enough that it responds well to the average properties of the acoustic wave in its vicinity. Additionally, a single short plate may be sufficient to do the necessary job. And, in any case, the couple is small enough and far enough from the walls that it is effectively an adiabatic element.

In the case of engines, the plates will usually be much longer to achieve effectively many elementary engines in series rather than the few suggested by Fig. 7; the plates will have a low longitudinal thermal conductance to reduce spurious heat leaks between the sources of hot and cold; there will be as many plates in parallel as possible, consistent with optimum efficiency; and the entropy flows at the ends of the plates will come from heat sources and sinks placed there for that purpose, rather than in steady state from the plates themselves. Furthermore, the concept of work flow and of steady longitudinal temperature gradient within the plates must be considered in addition to entropy flow. These new concepts, in addition to the qualitative

This article is copyrighted as indicated in the article. Reuse of AAPT content is subject to the terms at: http://scitation.aip.org/termsconditions. Downloaded to IP: 95.68.109.7 On: Wed, 23 Apr 2014 04:24:23

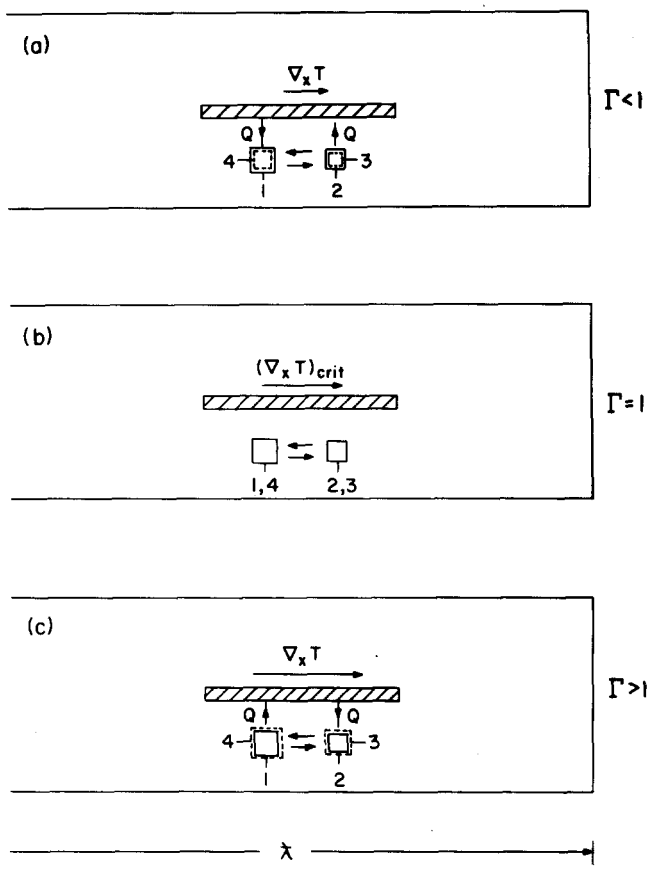

Fig. 8. Schematic diagram illustrating the thermodynamic effects of a longitudinal temperature gradient $\nabla_x T$ in a plate placed near the end of a resonant acoustical tube containing a zero Prandtl number fluid. To simplify the discussion in the text, the assumption is made that the plate length is small compared with its mean distance from the closed end, which in turn is small compared to λ. The three cases shown correspond to three values of $\Gamma \equiv (\nabla_x T)/(\nabla_x T)_{crit}$ [Eq. (13)]. In each case, a parcel of fluid located within the thermal penetration depth is shown as a square and imagined to go through an articulated cycle 1→2→3→4→1→. . . just as in the example of Fig. 7. Note that the volume of the parcel is shown explicitly to change as the cycle proceeds. The label Q with associated arrow indicates both the presence and direction of heat flow between fluid and plate during the slowly moving parts of the cycle. For $\Gamma < 1$, (a), the heat flows are reversed compared with the case $\Gamma > 1$, (c); and for $\Gamma = 1$, (b), there is no heat flow at all between parcel and plate.

effect of a longitudinal temperature gradient on the entropy flow, may be understood by reference to Fig. 8. Here we imagine a single plate with both its length and its distance from the closed end of a resonant tube small compared to the radian length λ. Some average temperature gradient $\nabla_x T$ is imposed on the plate in the direction shown. Again, to facilitate understanding, we imagine a single parcel of fluid undergoing the articulated cycle 1–2–3–4–1–· · · and assume that it lies within a thermal penetration depth of the plate so that fluid and plate communicate thermally. For purposes of explanation, we will assume that the processes 2→3 and 4→1 are essentially at constant pressure. We will further assume that longitudinal conduction is small and that $\nabla_x T$ is maintained by suitable sources and sinks of heat at the ends.

In case (a), the fluid is compressed and warmed adiabatically from 1 to 2. As there is now an impressed $\nabla_x T$, the difference in temperature between the fluid and the plate is reduced compared to the case $\nabla_x T = 0$, so less heat flows and the fluid entropy decreases by a smaller amount than for the case $\nabla_x T = 0$. From 2→3 the dynamic pressure is positive. As heat flows out, the size of the parcel diminishes. Hence, work is done on the parcel. In the process 3→4, a diminished entropy defect, compared to $\nabla_x T = 0$, is carried to the left. At 4, the temperature difference between fluid and plate is less than for the case $\nabla_x T = 0$, so the heat flow to the fluid is less and its entropy increase less. As a consequence, a diminished entropy increment, compared to $\nabla_x T = 0$, is carried to the right. From 4→1, the dynamic pressure is now negative while heat flow from the plate causes the fluid to expand. Hence, work is again done on the parcel. Summing up, in one cycle entropy has been caused to flow from left to right and work has been done on the fluid, though for both effects the quantities are *less* than they would have been for $\nabla_x T = 0$.

An interesting and important point that can already be seen, at least if the plate is not too long, is that while for a fixed $\nabla_x T$, the entropy flow does not depend on the length of the plate, the work flow is just linearly proportional to the amount of gas effectively exchanging heat with the plate. Hence, the work flow increases in proportion to the length of the plate. The direction of the work flow due to the plate's presence is from left to right.

It follows directly from the previous thinking that as the longitudinal temperature gradient $\nabla_x T$ imposed on the plate is increased even further it can reach a value such that the adiabatic temperature change of the fluid on moving from 1→2 is matched exactly by the change of the static temperature of the plate in the distance the fluid moved from 1 to 2. In this case, shown in Fig. 8(b), there is no temperature difference between fluid and wall, no heat flow, and no entropy change of the fluid. The same can be said for the absence of thermal effects following the process 3→4. Hence, for this particular longitudinal temperature gradient, which we call the critical temperature gradient $(\nabla_x T)_{crit}$, there is neither entropy flow nor work flow in one cycle. It is clear from the foregoing that application of acoustic power to a stack cannot pump up a temperature gradient greater than $(\nabla_x T)_{crit}$.

In Fig. 8, we have defined a quantity Γ such that

$$\Gamma \equiv (\nabla_x T)/(\nabla_x T)_{crit}. \tag{13}$$

Both a heat pumping function toward the closed end and a work flow toward the closed end as a consequence of introducing the plate correspond to $\Gamma < 1$. At $\Gamma = 1$, both stop. But as the temperature gradient can be imposed by sources of hot and cold at the ends of the plates we can impose $\Gamma > 1$, so that the temperature gradient exceeds critical. This is illustrated in Fig. 8(c) where the same line of reasoning used in analyzing Fig. 8(a) leads to a reversal of the direction of heat flow to and from the plate, a consequent reversal in the direction of entropy flow (now from right to left), and a reversal in the sign of the work flow so that work now is done by the fluid parcels and flows out of the plate. If Γ is made sufficiently large so that the work flow generated by the plates can overcome losses, then the acoustic system will oscillate spontaneously, as is required of a prime mover.

C. Understanding the various quantities on which the behavior of our thermoacoustic heat engines depends

In this section we want to develop, heuristically, formulas for heat flow and work flow in terms of the quantities

This article is copyrighted as indicated in the article. Reuse of AAPT content is subject to the terms at: http://scitation.aip.org/termsconditions. Downloaded to IP: 95.68.109.7 On: Wed, 23 Apr 2014 04:24:23

describing the fluid, the geometry of the engine, and the acoustics, again in the limit of vanishingly small Prandtl number. The heat flow we want to estimate is convective or hydrodynamic in nature and is obtained simply by multiplying the hydrodynamic entropy flow by the local temperature T_m. We are not interested at this point in numerical factors of order unity. The entropy transferred per cycle is estimated, for example, by the fluid's entropy change in the parts 2→3 or 4→1 of the cycles illustrated in Fig. 8. The entropy increment per unit mass from right to left is thus approximately

$$\Delta S \simeq \frac{c_p}{T_m} T_{1_{ad}} (\Gamma - 1) = \frac{c_p}{T_m} \frac{T_m \beta}{\rho_m c_p} p_1 (\Gamma - 1), \tag{14a}$$

where the effective temperature difference driving the heat flow between fluid and plate is the adiabatic temperature difference , Eq. (4), modified by the factor $(\Gamma - 1)$, see Eq. (13), which describes how the actual temperature difference between fluid and plate has been changed fractionally by the presence of a static temperature gradient in the plate, the sign being chosen to make entropy flow from hot to cold positive. The steady entropy flow is then given dimensionally by a formula

$$\dot{S} = \rho_m \dot{V} \Delta S, \tag{14b}$$

where $\dot{V}$ is a volume velocity which we write as

$$\dot{V} \simeq \Pi \delta_\kappa u_1, \tag{14c}$$

where Π is the perimeter of the plate for sections perpendicular to the flow, so that $\Pi \delta_\kappa$ is that part of the fluid cross section which is "on speaking terms" thermally with the plate. Combining (14a), (14b), and (14c) and multiplying by T_m, one then reaches the estimate for the time-average hydrodynamic heat flow

$$\dot{Q} \simeq \Pi \delta_\kappa (T_m \beta)(\Gamma - 1) p_1 u_1. \tag{15}$$

(For sinusoidal motion, the correct numerical factor in front of the right-hand side is 1/4.) This is actually quite a sensible approximate formula. The factor $T_m \beta$ is the thermodynamic quantity (unity for the ideal gas and 0.28 for liquid sodium near 700°C) which determines isothermal heat flow for a given pressure change. The quantity $(\Gamma - 1)$ is the factor, zero when $\nabla_x T = (\nabla_x T)_{crit}$, by which the average entropy flow from right to left is changed as the imposed longitudinal temperature gradient in the plate is changed. The area $\Pi \delta_\kappa$ is that part of the cross-sectional area of the fluid which partakes in the thermal action. The product $p_1 u_1$ is not unexpected empirically on the basis of the TAC data, Fig. 2, which show a zero output when either p_1 or u_1 is zero and a maximum where $p_1 u_1$ is maximum.

Yet another useful result is one for the critical temperature gradient in the plate. Aside from definition of sign, in a $\sigma = 0$ fluid this will always be equal to

$$(\nabla_x T)_{crit} = T_{1_{ad}} / x_1, \tag{16}$$

as $T_{1_{ad}}$ is just the fluid's adiabatic temperature change when it moves by amplitude x_1: if $x_1 (\nabla_x T) = T_{1_{ad}}$ the plate and the fluid will always have the same temperature laterally and no heat will flow between them. If the plate is located near the closed end and the plate sectional area is small compared to the total area, $(\nabla_x T)_{crit}$ has a particularly simple form as in that case, ignoring algebraic sign,

$$x_1 \simeq x_m k_s p_1 \quad (x_m \ll \lambda), \tag{17}$$

where x_m is the distance of the point on the plate from the closed end of the tube. Hence, using Eqs. (4) and (6), one finds for the magnitude of the critical temperature gradient

$$(\nabla_x T)_{crit} = \frac{\gamma - 1}{T_m \beta} \frac{T_m}{x_m}, \quad (x_m \ll \lambda). \tag{18}$$

Aside from the dimensionally expected ratio T_m / x_m the quality of the fluid that is important is the ratio of the work parameter $(\gamma - 1)$ to the heat parameter $(T_m \beta)$.

One can also see from Eq. (16) and its context that even though T_1 may be small, perhaps a degree or so, the total temperature difference across the plates at critical temperature gradient can be quite large simply because the length of the plates may be many times x_1.

Next let us estimate the work flow resulting from the presence of the plates in a geometry such as is shown in Fig. 9. To the right of the plates is an open space in which we will assume for simplicity that all processes are adiabatic. The time average work flow that we wish to calculate is, at any particular value of x,

$$\overline{\dot{W}} = \overline{p_1 \dot{V}_1}, \tag{19}$$

where $\dot{V}_1$ is the volume velocity of the fluid at that point and the bars indicate time average. The product of the cross-sectional area of the fluid and the fluid velocity u_1 is $\dot{V}_1$. Now for the adiabatic processes to the right of the plates, all of the displacement x_1, the dynamic pressure p_1, and the dynamic temperature T_1 are in time phase. Thus u_1 leads p_1 by 90° in time phase, and the time average $\overline{\dot{W}}$ in Eq. (19) is zero. This is a reasonable result. But the introduction of the plates, owing to the irreversible process of thermal conduction, changes the phase of u_1 with respect to p_1. Let us estimate the magnitude of $\dot{v}_1$, the component of $\dot{V}_1$, which is not in quadrature with p_1. Dimensionally, $\dot{v}_1$ is of the form

$$\dot{v}_1 = \omega V k_{eff} p_1, \tag{20a}$$

where V is some volume and k_{eff} some compressibility that we will estimate heuristically. The value we put down for V depends on where we want to compute $\overline{\dot{W}}$. V will increase from zero adjacent to the adiabatic space to

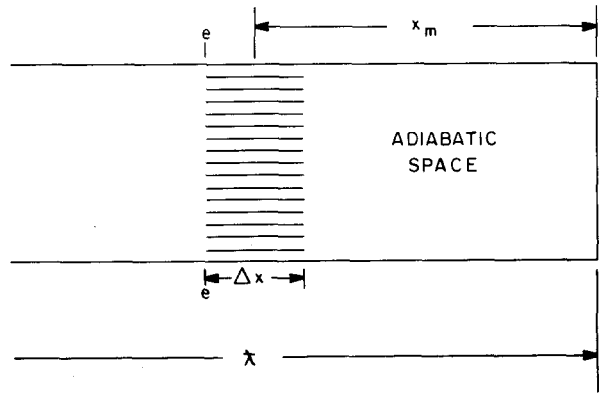

Fig. 9. Model of a set of parallel plates of length Δx set at a mean distance x_m from the end of an acoustically resonant tube containing a zero Prandtl number fluid. In the text, for simplicity, we have taken $\Delta x \ll x_m \ll \lambda$. The end of the plates labeled e–e is defined to be the exit from the stack of plates; and the space to the right of the plates is taken to be adiabatic, which is equivalent to the assumption that the wall area there is negligible compared to that of the plates.

This article is copyrighted as indicated in the article. Reuse of AAPT content is subject to the terms at: http://scitation.aip.org/termsconditions. Downloaded to IP: 95.68.109.7 On: Wed, 23 Apr 2014 04:24:23

$\Pi\delta_\kappa \Delta x$ at the exit e–e, Fig. 9, from the plates, where Π is the total perimeter of the stack of total length Δx. Hence, if $\bar{\dot{W}}$ is to be computed at the "exit" from the stack, we have

$$V \simeq \Pi\delta_\kappa \Delta x. \tag{20b}$$

The effective compressibility k_{eff} is somewhat more subtle to estimate. First of all, the shift in phase of u_1 with respect to p_1 results because, even after a pressure maximum, say, gas continues to flow from the left into the plate region as heat is transferred from gas to plate. The effective compressibility thus depends in part on the *difference* $(k_T - k_s)$ between the isothermal and adiabatic compressibilities. But in the presence of an imposed longitudinal temperature gradient in the plates the temperature differences that cause the heat flows that lead to the phase shifted gas motion are changed fractionally by the factor $(\Gamma - 1)$, just as in the hydrodynamic heat flow case above. Hence for k_{eff} we write

$$k_{\text{eff}} \simeq (k_T - k_s)(\Gamma - 1) = (\gamma - 1)k_s(\Gamma - 1), \tag{20c}$$

where the second form is a consequence of using Eq. (6), and where the sign of $(\Gamma - 1)$ is taken so that a positive $\bar{\dot{W}}$ will correspond to a work flow from right to left. Now replace k_s in Eq. (20c) with $(\rho_m a^2)^{-1}$ from Eq. (1). Substitute for p_1 in Eq. (20a) a value of u_1 derived from the relation, valid for $x/\lambda \ll 1$, $u_1 \simeq (p_1/\rho_m a)(x_m/\lambda)$, and use $\omega\lambda = a$. Then Eqs. (19) and (20a)–(20c) give the result for the average work flow

$$\bar{\dot{W}} \simeq \Pi\delta_\kappa(\gamma - 1)(\Gamma - 1)p_1 u_1 \Delta x / x_m. \tag{21}$$

(For sinusoidal motion, the correct numerical factor in front of the right-hand side is 1/4.) This very interesting result should be compared with the heat flow formula of Eq. (15). The work parameter $(\gamma - 1)$ replaces the heat flow parameter $(T_m\beta)$. For helium gas $\gamma - 1 = 2/3$; for liquid sodium at 700°C, $\gamma - 1 = 0.43$. The quantities $\Pi\delta_\kappa$ and $(\Gamma - 1)$ occur in both formulas for the same reason. Both flows are proportional to the $p_1 u_1$ product. But the work flow has an additional factor $\Delta x/x_m$, as it must intuitively since the work flow must be proportional to the amount of gas in effective thermal contact with the plates.

D. Efficiency of the acoustic engine

Now if the numerical factors preceding the estimates for $\bar{\dot{Q}}$ and $\bar{\dot{W}}$ as given in Eqs. (15) and (21) are the same, and this turns out to be the case, then for relatively short plates $\bar{\dot{W}}$ will be small compared to either of the heat flows at the ends of the plates, which can thus be taken to be essentially the same for present purposes. Then the efficiency η of this ideal acoustic engine is simply the ratio of Eq. (21) to Eq. (15) or

$$\eta = \frac{(\gamma - 1)}{T_m\beta}\frac{\Delta x}{x_m}. \tag{22}$$

This truly remarkable result says that the efficiency (or for $\Gamma < 1$ the coefficient of performance) of the engine depends on the *geometry* or configuration of the engine and also on some thermodynamical properties such as $(\gamma - 1)$ and $(T_m\beta)$. The actual temperature gradient imposed on the engine does not appear at all: specify the fluid and the mean temperature so that $(\gamma - 1)$ and $T_m\beta$ are known and you know the efficiency from the engine's configuration. This may be one of the very special properties of a "natural engine."

Of course it is always possible to introduce the concept of temperature into an equation like Eq. (22). Simply note that Δx is just the ratio of the imposed temperature difference ΔT and the imposed gradient dT_m/dx and use Eq. (18) to write $(\gamma - 1)/(T_m\beta)x_m = (\nabla_x T)_{\text{crit}}/T_m$, and one can rewrite Eq. (22) as

$$\eta = \frac{\Delta T}{T_m}\frac{(\nabla_x T)_{\text{crit}}}{(\nabla_x T)}. \tag{23}$$

Within our approximations the Carnot efficiency is $\eta_C \simeq \Delta T/T_m$, so using the definition of Γ, Eq. (13), one can further rewrite the efficiency equation as

$$\eta = \eta_C/\Gamma \quad (\Gamma > 1). \tag{24}$$

Now as Γ approaches unity, both heat flow rates and work flow rates approach zero, as we described in Sec. V B above. Equation (24) shows that under these conditions η approaches the Carnot efficiency, which is a very reasonable result. For $\Gamma < 1$ we no longer have a prime mover but rather a heat pump, so the concept of efficiency has to be replaced by that of coefficient of performance. Then the coefficient of performance COP obeys the formula

$$\text{COP} = (\text{COP})_C\Gamma \quad (\Gamma < 1). \tag{25}$$

No matter whether the ideal engine does external work or pumps heat, it has a performance which depends on geometry or configuration. If compared with a Carnot engine, the performance is inferior by a factor which is given by the ratio of the impressed temperature gradient to the critical temperature gradient.

VI. SIMPLE QUANTITATIVE RESULTS

As we indicated at the outset, most thermoacoustic phenomena are quantitatively complex, so that both an intricate theory and detailed numerical computation with the theory are necessary to make a comparison between experiment and theory. A notable exception is the thermoacoustic couple (TAC), where excellent agreement has been obtained[21,22] between experiment and simple theory. The essential point is that the typical TAC has just a few small widely spaced plates so that its impact on the sound field in the absence of the TAC is small. But in an engine, the objective is to have enough of the acoustically active volume filled with plates so that there is a major impact on the acoustic field within the plates.

The theory of the TAC has been worked out in detail in Ref. 22, Sec. II. The result for the time-averaged hydrodynamic heat flow associated with the couple in a gas $(T_m\beta = 1)$ is

$$\bar{\dot{Q}}_2 = -\frac{\Pi}{4}u_\infty p_1\delta_\kappa\left(\frac{1-\sqrt{\sigma}}{1+\sigma}\cos\phi - \frac{1+\sqrt{\sigma}}{1+\sigma}\sin\phi\right) - \frac{\Pi}{4}u_\infty^2\delta_\kappa\frac{\rho_m a^2\Theta}{\omega(\gamma-1)}\frac{1-\sigma\sqrt{\sigma}}{1-\sigma^2}, \tag{26}$$

where the subscript 2 on $\bar{\dot{Q}}$ indicates that the theory is valid to second order in small quantities, u_∞ is the amplitude of the acoustic velocity far from a plate, ϕ is the angle by which the acoustic velocity far from the plate leads the dynamic pressure, and $\Theta \equiv T_m^{-1}\,dT_m/dx$ is the logarithmic temperature gradient in the plates. As the couple is short and nonintrusive, p_1, u_∞, and ϕ will be given with adequate accuracy by their values in a lossless resonant tube occupying the space $x > 0$ and with the tube closed at

This article is copyrighted as indicated in the article. Reuse of AAPT content is subject to the terms at: http://scitation.aip.org/termsconditions. Downloaded to IP: 95.68.109.7 On: Wed, 23 Apr 2014 04:24:23

$x = 0$:

$$p_1 = P_0 \cos(\omega x/a), \tag{27}$$

$$u_\infty = (P_0/\rho_m a)\sin(\omega x/a), \tag{28}$$

and

$$\phi = -\pi/2. \tag{29}$$

The second term in (26) can be neglected for low induced temperature gradients, leading to a highly sinusoidal (but with half the acoustic wavelength) dependence on x, as demonstrated in Fig. 2.

If the couple is small enough and of high enough internal thermal conductance that it is effectively isolated from its surroundings, then one can write $\dot{\bar{Q}}_2 - kA\, dT/dx = 0$ for all points along the couple, where k is the thermal conductivity and A is the sectional area of the solid plate. If further the couple is quite short one can replace $\dot{\bar{Q}}_2$ by its spatial average $\langle \dot{\bar{Q}}_2 \rangle$ and dT/dx by $\Delta T/l$, where l is the effective length of the couple and ΔT is the temperature difference across it. Then one has for the temperature difference expected across the couple

$$\Delta T = \langle \dot{\bar{Q}}_2 \rangle / (kA/l), \tag{30}$$

where $\langle \dot{\bar{Q}} \rangle$ is evaluated from Eq. (26) using the thermophysical properties of the gas and using Eqs. (27)–(29) to evaluate p_1, u_∞, and ϕ for the value of x corresponding to the average position of the couple. P_0 is of course a primary measured quantity. As we pointed out in Ref. 22 the most uncertain quantity is kA/l, the effective "conductance" of the couple, as both the epoxy-impregnated graph paper and the gas surrounding the couple will contribute. We analyzed the data of Fig. 2 as outlined above using the appropriate properties of air and concluded that the data would be explained if *all* the conduction were in the solid material and its thermal conductivity were 4.5 mW/cm K. This is to be compared with thermal conductivities of epoxy resin, fiberglass, and air of 2, 8. and 0.26 mW/cm K, respectively. In reality, about 1/3 of the return diffusive heat was probably carried by the air owing to its larger cross section for heat transport. In any event, the agreement between observations and theory is reasonable. We think even at this level of quantitative work that experiments with the TAC could form a very useful and stimulating basis for experiments in senior physics laboratories. The apparatus is simple and inexpensive and involves acoustics and acoustical techniques in which many students are very interested. The effects are novel. And understanding the phenomena in any depth requires a working knowledge of heat and thermodynamics, which should help to stimulate interest in senior physics courses in this area.

VII. SOME QUANTITATIVE OBSERVATIONS ON THE ACOUSTIC OSCILLATOR

When the acoustic oscillator of Fig. 3 has been instrumented as indicated in Sec. III to allow both accurate measurements of dynamic pressure at the closed end and temperature measurements across the plates, a number of rather interesting measurements of semiquantitative value can be made. To define the conditions somewhat better, we insulated crudely the open-ended copper tube, used a heating tape to maintain the closed-ended copper tube near room temperature of about 23°C, and bolted a heavy copper plate transverse to the cold end of the engine flange and inserted it in liquid nitrogen at an appropriate level to allow roughly constant temperature to be imposed on each of the open-ended and closed-ended copper tubes. Then we made two types of observations, in both types the closed end being maintained near room temperature. In one we set up an initial temperature ratio across the plates but with the open end blocked by a thermally insulating plate. (In this condition the lowest resonance would have the engine plates at the quarter wavelength position so that they could not drive oscillations.) Then the plate was suddenly removed and photographs of the oscillating pressure at the closed end obtained as a function of time using an oscilloscope. Example of these data are shown in Fig. 4(a) and 4(b). The largest "steady-state" amplitude and most rapid rises to "steady state" were achieved for the lowest temperature imposed initially on the open tube. (These "steady state" amplitudes eventually change with time as the temperature difference across the plates changes; see below.) As the temperature T_C was allowed to increase both the rate of rise and the final "steady state" amplitude decreased, until finally no oscillation could be detected at all. During the time that the photographs were being taken, the change of temperature across the plates as measured by the thermocouple attached to the copper strips was generally very small. Examples of the development of oscillation amplitude with time for several cases are shown in Fig. 10, where $\ln P_0$ is plotted linearly against time interval, the zero of time interval having no significance. The initial "hot" temperature in all cases is ca. 295 K. The initial rise of P_0 is rather accurately exponential. The initial slopes $d \ln P_0/dt$ were computed from data of this sort and plotted in Fig. 11 as a function of $\ln (T_H/T_C)_i$ where $(T_H/T_C)_i$ is the initial value of the ratio of hot to cold temperatures.

Some features of Figs. 10 and 11 are quite reasonable while others suggest that probably both the experiments

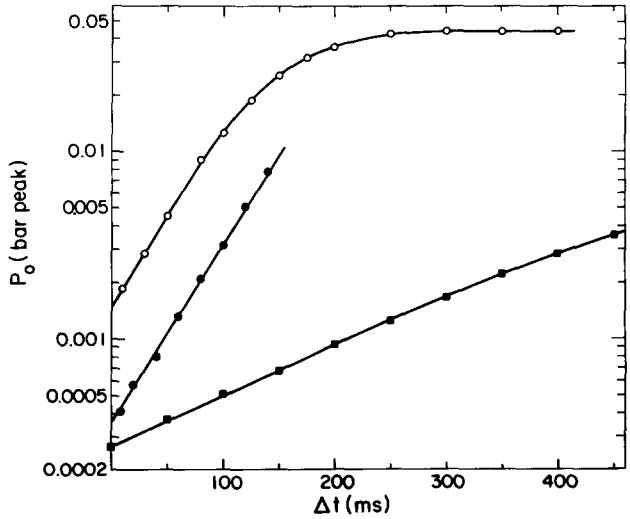

Fig. 10. Plots of representative data, such as those shown in Fig. 4, for the buildup of acoustic oscillations in the heat-driven oscillator of Fig. 3. The amplitude of the dynamic pressure amplitude P_0 at the closed end is plotted on a logarithmic scale against a time interval, with arbitrary zero, plotted linearly. The initial growth of P_0 is exponential within the precision of the measurements. The three sets of data shown correspond to three values of the initial temperature ratio, $(T_H/T_C)_i$: ○, 2.86; ●, 2.74; ■, 1.82. Triggering for the data with open circles was arranged to illustrate the initial saturation of P_0 with Δt. The gas is air at 0.78 bar, $T_H \simeq 295$ K, and the frequencies represented are, for example: ●, 193 Hz; ■, 226 Hz.

This article is copyrighted as indicated in the article. Reuse of AAPT content is subject to the terms at: http://scitation.aip.org/termsconditions. Downloaded to IP: 95.68.109.7 On: Wed, 23 Apr 2014 04:24:23

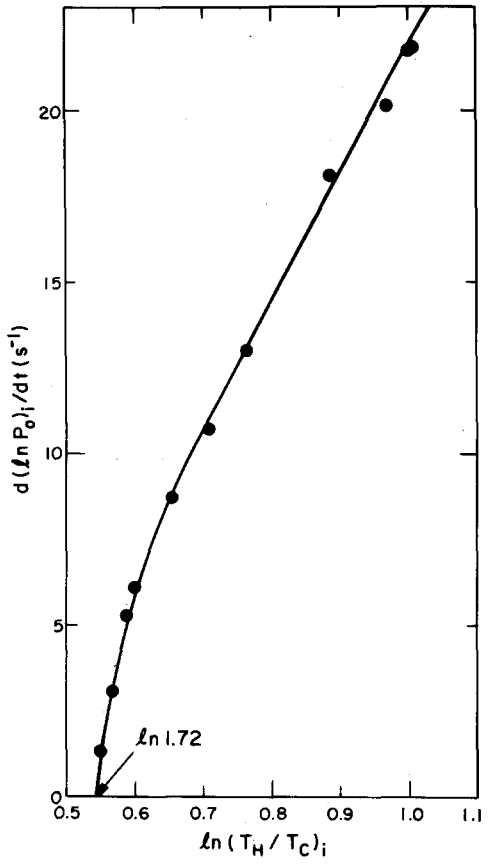

Fig. 11. Variation of the initial slope $(d \ln P_0/dt)_i$ with the natural logarithm of the initial temperature ratio $(T_H/T_C)_i$ across the plates of Fig. 3 for a variety of data in addition to those shown as examples in Fig. 10. The data suggest that for $(T_H/T_C)_i$ near 1.72 or below acoustical oscillations will not occur spontaneously in the device of Fig. 3. The gas is air, and $T_H \simeq 295$ K.

and our model of what is happening are too crude at this stage. With respect to the buildup of oscillations from zero, the following comments can be made. First, the argument for the work flow from the engine plates leading to the heuristic result (21), valid for $\sigma = 0$ and small temperature differences, will have to be modified both because $\sigma \simeq 0.70$ for air and because the temperature ratio T_H/T_C is not close to unity. Furthermore, the thermophysical properties, such as κ and ν, will also be functions of position. As for gases we have $T_m\beta = 1$, Eq. (18) for the critical temperature gradient could also have been written

$$\left(\frac{d \ln T_m}{dx}\right)_{\text{crit}} = \frac{\gamma - 1}{x_m}, \tag{31}$$

so it is not surprising that in a more complete theory Γ of Eq. (13) would be replaced by

$$\Gamma' \equiv \frac{d \ln T_m dx}{(d \ln T_m/dx)_{\text{crit}}}. \tag{32}$$

Certainly we can expect the overall work flow to be proportional to the product $p_1 u_1$ at the plates, and as both are proportional to the dynamic pressure amplitude P_0 measured at the closed end we should expect that the average work flow $\overline{\dot{W}}_e$ produced by the engine would have the form

$$\overline{\dot{W}}_e = \alpha(\Gamma' - 1)P_0^2, \tag{33}$$

where α is a proportionality factor that will vary with the temperature and mean pressure conditions imposed on the engine. In order to produce spontaneous oscillations, the work flow from the engine must overcome all the losses, including both the viscous and pressure induced thermal conduction losses within the tube and the acoustic radiation loss from the end of the tube. All of these, for a given set of average thermal conditions will be proportional to P_0^2. Following Morse,[28] the acoustic power radiated from the end of the tube is

$$\overline{\dot{W}}_a = \frac{1}{8}\frac{P_0^2 a \pi r_1^4}{\gamma p_m \lambda^2}, \tag{34}$$

where r_1 is the radius of the open end of the tube and $r_1 \ll \lambda$. Using this formula we have estimated that the maximum acoustic power emitted by the oscillator is of order 20 mW. In any event, we can expect that the total rate of loss of energy is of the form

$$\overline{\dot{W}}_L = \xi P_0^2, \tag{35}$$

where ξ is another proportionality factor that can be expected to depend on the temperature distribution within the tube.

Now if $\overline{\dot{W}}_e$ exceeds $\overline{\dot{W}}_L$ we can expect oscillations to build up once some fluctuation occurs to get them started. At first, the excess of $\overline{\dot{W}}_e$ over $\overline{\dot{W}}_L$ will be used to increase the average acoustic energy $\overline{W}_S$ stored in the tube, a quantity which is also proportional to P_0^2:

$$\overline{W}_S = \epsilon P_0^2, \tag{36}$$

with $\epsilon \simeq (1/4)\pi r_1^2 l/\gamma p_m$, where $\pi r_1^2 l$ is the effective volume of the tube. Thus, for that period of time in which the heat capacities of the solid parts assure that the temperature distributions do not change, we can expect by conservation of energy that

$$\epsilon \frac{d}{dt} P_0^2 = \alpha(\Gamma' - 1)P_0^2 - \xi P_0^2, \tag{37}$$

using all of (33), (35), and (36). This can be rewritten in a form to motivate the plot of Fig. 10 and justify the observed initial linear variations observed there:

$$\frac{d \ln P_0}{dt} = \frac{1}{2\epsilon}[\alpha(\Gamma' - 1) - \xi]. \tag{38}$$

It is essential that the quantity in square brackets in (38) exceed zero for oscillations to occur. The plot of the experimental values of the left side of (38) versus $\ln(T_H/T_C)_i$ [with the logarithm used as suggested from (32) and $\Delta \ln T_m/\Delta x \propto \ln T_H/T_C$] given in Fig. 11 shows that some or all of the quantities on the right side of (38) depend on the temperature distribution, even suggesting a phenomenon like critical slowing down. The accurately linear dependence of $\ln P_0$ on time interval during the initial buildup suggests that the general approach is correct. Two other points about Fig. 11 should be noted. One is that the data extrapolate crudely to a critical temperature ratio for oscillations to start of $T_H/T_C \simeq 1.72$, which is in rough agreement with estimates of this quantity. The second is that the slope of Fig. 11 for the larger values of $\ln(T_H/T_C)_i$ is about 27 s^{-1} while a crude theory taking into account the temperature dependence of the various quantities in α and β had suggested 20 s^{-1} for this number.

Another question regarding the observations is concerned with that quality which determines the equilibrium amplitude of the oscillations, as shown both in Fig. 4(b) and

This article is copyrighted as indicated in the article. Reuse of AAPT content is subject to the terms at: http://scitation.aip.org/termsconditions. Downloaded to IP: 95.68.109.7 On: Wed, 23 Apr 2014 04:24:23

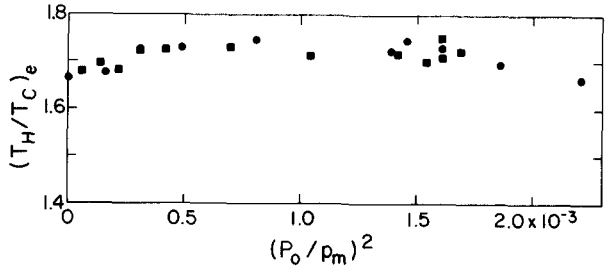

Fig. 12. Relationship between the equilibrium temperature ratio $(T_H/T_C)_e$ across the plates of the thermal oscillator of Fig. 3 and the square of the ratio of the dynamic pressure amplitude P_0 of the sound produced to the mean pressure p_m. The different values of P_0 are obtained by maintaining the closed copper tube near $T_H \simeq 295$ K and by varying the temperature of the open (and crudely insulated) copper tube. The gas is air. The highest peak-to-peak sound amplitude at the closed end represented here is 9.4% of the atmospheric pressure of 0.78 bar.

in the top curve of Fig. 10. Certainly one possibility is the presence of higher order terms than the second used in the previous discussion. But our experiments suggest, at least up to the rather substantial amplitudes observed thus far, quite a different explanation. In a given observation the mouth of the oscillator was closed with an insulating plate to prevent oscillations, the initial temperature T_H of the closed end was adjusted to be near 295 K, and by adjustment of the liquid N_2 level on the thermal contact plate (see comments on geometry both at the beginning of this section and in Sec. III) the initial temperature T_C of the cold end of the engine stack could be adjusted. For the present observations, the insulating plate was then removed, the transient behavior shown in Figs. 4 and 10 allowed to occur, and then both oscillation amplitude and the temperatures T_H and T_C at the ends of the plate observed as a function of time until a steady state was reached. These steady-state temperature ratios $(T_H/T_C)_e$ are plotted as a function of the corresponding values of $(P_0/p_m)^2$ in Fig. 12. The mean pressure p_m was 0.782 bar, local atmospheric pressure, for these data. The acoustic intensity is proportional to P_0^2. The remarkable quality of these data is that $(T_H/T_C)_e$ is almost independent of the acoutic intensity over a very wide range and on the average about the same, within experimental error, as the crudely extrapolated value of 1.72 found in the data depicted in Fig. 11. There is a drop in $(T_H/T_C)_e$ both at very low and very high intensity. The former may reflect the onset of importance of ordinary longitudinal diffusive conduction as the hydrodynamic heat flows diminish. The latter may reflect a competition between the effects of thermal conduction in the copper thermal contact strips, which tend to reduce the measured $(T_H T_C)_e$ compared to the average value of the quantity, and effects of phenomena such as acoustic streaming[29] which may increase losses and hence tend to increase $(T_H/T_C)_e$. Examination of Eq. (37) shows that to second order there is no effect to limit the oscillation amplitude. What the data of Fig. 12 suggest to us is that, for the oscillation amplitudes produced in our experiments, the equilibrium acoustic intensity is determined simply by the rate at which heat can be supplied to and extracted from the ends of the plates through the thermal resistances between the ends of the plates and the sources of heat and cold. The actual temperature ratio across the plates remains, meanwhile, very near to the critical value just needed to sustain oscillations. This will be a very interesting point to study in depth in the future.

VIII. GENERAL REMARKS

The thermoacoustic engines whose properties we have decribed by experimental example and heuristic explanation are a subclass of a more general type of engine which we like to call "natural engines." Certain qualities of the thermoacoustic engine can be appreciated readily in Figs. 7–9. Here we have two thermodynamic mediums: a primary, which is the fluid; and a secondary, which is the adjacent solid material. These two have a reciprocating motion with respect to one another. Accompanying this motion is a thermodynamic effect, in this case a temperature change accompanying the pressure change. There is an exchange of energy between the two mediums, in this case a flow of heat, due to a natural irreversible process, in this case the conduction of heat across a nonzero temperature difference. The irreversible process leads to a time-phase change between the motion and the thermodynamic effect, which is essential for the existence of some net thermodynamic effect in a cycle. Additionally, the second medium has ends, and these are the places where energy is added to or removed from the primary medium. Examination of the cause of these energy flows at the ends shows that they are a consequence of changes in the relative energy-related environment or interaction of the two mediums. For the lack of a more descriptive term, we have said that the thermodynamic symmetry has been broken at the ends.

It is clear from the above description that the qualities of such engines are not limited as to material or to time scale. The primary and secondary mediums may be interpenetrating, rather than side by side, and they may be electrically charged as well as neutral. The thermodynamic effect may involve change of phase (e.g., liquid $\leftrightarrow$ solid) rather than only processes within a single phase. It is also probable in a broader class of natural engines that the concept of heat itself need not play a major role.

In engines in the same subclass as thermoacoustic engines, there are also the concepts both of an "ideal engine" of this type, in which the irreversible process of friction is negligible; and of a critical temperature gradient along the direction of reciprocating motion, or a region of such gradients, which separate the functions of heat pumping (work$\rightarrow$ heat transfer) and prime moving (heat transfer$\rightarrow$ work). Another remarkable quality of the natural engines we have studied can be seen by examining Fig. 9. The thermoacoustic engine is really a number of small engines in series whose ultimate sources and sinks of energy are at the ends. Now the *heat* flow from one of the reservoirs generally depends on one length, of order x_m, while the work flow is roughly proportional to Δx. Hence either the efficiency or coefficient of performance of the engine depends on the ratio of these quantities. They depend on the geomentry and configuration of the engine, as well as, of course, on quantities typifying the materials involved.

The above properties may prove useful in the future both as models and as paradigms to aid in understanding both process and function in diverse systems.

ACKNOWLEDGMENTS

We wish to acknowledge here the many contributions of S. L. Garrett and L. J. Campbell to the experimental, con-

This article is copyrighted as indicated in the article. Reuse of AAPT content is subject to the terms at: http://scitation.aip.org/termsconditions. Downloaded to IP: 95.68.109.7 On: Wed, 23 Apr 2014 04:24:23

ceptual, and calculational aspects of our work in thermoacoustics and, as well, a fruitful correspondence with N. Rott. We are grateful for the continued help and encouragement of W. E. Keller.

APPENDIX

It may be useful to those interested in developing their own simple thermoacoustic models, to have a few more details of some of the apparatus described above. In Fig. 13, we show a composite photograph of (a) the thermoacoustic couple used to obtain the measurements of Fig. 2, (b) a typical fiberglass engine plate and copper thermal-contact strip used in the thermal oscillator, Fig. 3, together with the assembled "engine," less closed and open tubes for that device, and (c) two representative stacks of fiberglass plates in a parallel-plate configuration such as could be used in an acoustic cooling engine. In examining (c), note that the stacks have been placed and lighted in such a way as to emphasize their "transparency" when viewed parallel to the planes of the plates.

Quantitative details on the cooling engine of Fig. 5 are as follows. The pressure vessel containing the driver consists of an aluminum cover plate, 1, with a central pipe-tapped hole, 2, for introducing the gas to be used and a bottom vessel and heat sink, 3. The driver (Dynaudio D-54, 2-in. dome mid-range, made in Denmark) consists of voice coil, 5, pole pieces, 6 and 6′, and magnet, 7, the whole being held firmly by aluminum driver clamp and heat sink, 4, to the pressure vessel, 3, by screws (not shown). A copper microphone flange, 8, provided a suitable cavity for a calibrated special Y-cut quartz microphone installed at M. The cloth dome of the commercial driver was cut off near the voice coil and replaced by a 0.5-mm wall aluminum driver cone (with a few 3-mm-ϕ holes in the conical surface) glued near the voice coil. A new surround, 9, was made from cloth and epoxy to provide the desired spring force and to seal between the aluminum driver cone and 8. These modifications are nontrivial and will be described in more detail in a subsequent publication.

The top part of the acoustic system consisted of a copper flange and extension, 10 (with knife edge at bottom for sealing to the epoxy fiberglass tube, 12). This part also was counterbored to receive the copper heat sink assembly, 11, thermal contact being made using Dow Corning 340 heat sink compound. Contact with the gas was made via a stack of four copper squaremesh screens (wires in the screens were on 1.25-mm centers) soldered along their periphery to part 11. (This whole heat sink arrangement needs substantial improvement.)

The second medium was made from a 244-cm-long $\times$ 82.4-mm-wide strip of 0.076-mm-thick DuPont Kapton H-Film sheet with straight transverse 0.38-mm-diam Nylon monofilament cylinders on 5–mm centers adhered to the Kapton using Scotch 77 spray adhesive (using a special jig and a stretcher to align the monofilaments precisely and adhere them in batches of 30 each). The resulting sheet was wound on a 6.4-mm-diam cloth phenolic rod, 13, out to a diameter of 38.1 mm, the i.d. of epoxy fiberglass tube, 12, which had a wall thickness of ca. 1.8 mm. The calculated total perimeter Π of S for entropy flow in the gas is ca. 488 cm.

The bottom of S is supported by a cross C made of thin stainless-steel sheet resting on the start of the necked-down region of the fiberglass, which itself is sealed to copper socket, 14, machined with a knife edge to facilitate the epoxy fiberglass seal. The thin-walled copper tube, 15, is soldered into copper socket, 14, and brass socket, 16. This tube has an i.d. of 22.1 mm and a wall thickness of 0.89 mm everywhere except at the sockets, where the wall thickness is 1.65 mm. The gas spring V is enclosed in a welded vessel of one liter volume whose ends, 18 and 18′, are made from 3.2-mm-thick stainless-steel plates and whose sidewall is a 101.6-mm-o.d. $\times$ 0.64-mm wall tube. The mass of this stainless-steel vessel was 605 g.

To provide necessary thermal insulation the bottom of 3 was sealed using an O–ring to a vacuum vessel and ca. 15 wraps of superinsulation were put around the entire device. Copper tubes for cooling water were also greased to the cylindrical surface of 3.

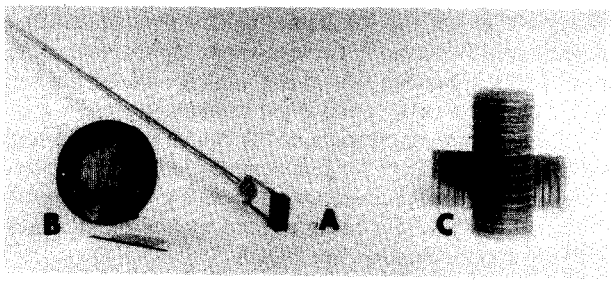

Fig. 13. Photograph of some of the parts used in thermoacoustic experiments. (a) The thermoacoustic couple shown as part of Fig. 1. (b) One fiberglass plate with a single adhered copper heat exchange strip in front of the engine assembly of the thermoacoustic oscillator of Fig. 3. (c) Two sets of parallel fiberglass plates which can be used in thermoacoustic cooling engines. These plates are 0.067 mm thick and spaced by 0.38 mm. During their rather complicated fabrication the plates were originally spaced by aluminum plates and epoxy impregnated. The whole was then turned to have a circular shape of outer diameter 37.7 mm about an axis parallel to the plane of the plates. The white rings and lines at the ends are epoxy impregnated cotton thread which has been epoxied into grooves machined into the outer surface to give added rigidity. The aluminum spacing plates contained 0.5-mm-diam holes placed on 6.5-mm centers and the whole vacuum impregnated with epoxy before the turning operation. This assured that the whole structure would be quite rigid once the aluminum spacers were etched out with diluted hydrochloric acid solution. The cylinders have been placed and lighted to emphasize their near transparency when observed from directions nearly parallel to the individual plates.

[1]A. A. Putnam and W. R. Dennis, J. Acoust. Soc. Am. **28**, 246 (1956).
[2]B. Higgins, Nicholson's J. **1**, 130 (1802).
[3]C. Sondhauss, Ann. Phys. (Leipzig) [2] **79**, 1 (1850).
[4]P. L. Rijke, Ann. Phys. (Leipzig) [2] **107**, 339 (1859).
[5]N. Rott, Adv. Appl. Mech. **20**, 135 (1980).
[6]K. W. Taconis, Physica **15**, 738 (1949).
[7]T. Yazaki, A. Tominaga, and Y. Narahara, J. Low Temp. Phys. **41**, 45 (1980).
[8]K. T. Feldman, Jr., J.Sound Vib. **7**, 71 (1968).
[9]W. E. Gifford and R. C. Longsworth, *International Advances in Cryogenic Engineering* (Plenum, New York, 1966), Vol. 11, p. 171.
[10]P. Merkli and H. Thomann, J. Fluid Mech. **70**, 161 (1975).
[11]J. W. Strutt (Lord Rayleigh), *The Theory of Sound* (Dover, New York, 1945), Vol. II, Secs. 322 f-i.
[12]N. Rott, Z. Angew. Math. Phys. **20**, 230 (1969).
[13]N. Rott, Z. Angew. Math. Phys. **24**, 54 (1973).
[14]N. Rott, Z. Angew. Math. Phys. **25**, 619 (1974).
[15]N. Rott, Z. Angew. Math. Phys. **26**, 43 (1975).
[16]N. Rott. and G. Zouzoulas, Z. Angew. Math. Phys. **27**, 197 (1976).

This article is copyrighted as indicated in the article. Reuse of AAPT content is subject to the terms at: http://scitation.aip.org/termsconditions. Downloaded to IP: 95.68.109.7 On: Wed, 23 Apr 2014 04:24:23

[17]G. Zouzoulas and N. Rott. Z. Angew. Math. Phys. **27**, 325 (1976).
[18]U. A. Müller and N. Rott, "Thermally Driven Acoustic Oscillations, Part VI: Excitation and Power" (preprint).
[19]J. Wheatley, Physica B **109** and **110**, 1764 (1982).
[20]J. Wheatley, "Intrinsically Irreversible Heat Engines," in *Proceedings of the "Near-Zero" Conference*, edited by C. W. F. Everitt (Freeman, San Francisco, in press).
[21]J. Wheatley, T. Hofler, G. W. Swift, and A. Migliori, Phys. Rev. Lett. **50**, 499 (1983).
[22]J. Wheatley, T. Hofler, G. W. Swift, and A. Migliori, J. Acoust. Soc. Am. **74**, 153 (1983).
[23]Radio Shack Cat. No. 40-1284C, 20-Watt, 8-Ω impedance.
[24]R. Stirling, "Improvements for Diminishing the Consumption of Fuel, and in Particular an Engine Capable of Being Applied to the Moving of Machinery on a Principle Entirely New," No. 4081, British Patent Office, London (1816).
[25]P. C. Allen, W. R. Knight, D. N. Paulson, and J. C. Wheatley, Proc. Natl. Acad. Sci. (USA) **77**, 39 (1980).
[26]P. H. Ceperley, J. Acoust. Soc. Am. **66**, 1508 (1979).
[27]G. W. Swift, A. Migliori, S. L. Garrett, and J. C. Wheatley, Rev. Sci. Instrum. **53**, 1906 (1983).
[28]P. M. Morse, *Vibration and Sound* (Acoustical Society of America, New York, 1982), p. 314.
[29]N. Rott, Z. Angew. Math. Phys. **25**, 417 (1974).

Queueing: A different model for physics

Gregory L. Baker
Academy of the New Church College, Bryn Athyn, Pennsylvania 19009

(Received 21 October 1983; accepted for publication 27 March 1984)

The analogy of simple queueing models with physical, two-level systems is described. Time-dependent and steady-state queues are used to model radioactive decay and spin systems, respectively. The queue model for the spin system is seen to predict (1) the average population difference between the energy levels when a small periodic magnetic field is applied, (2) the relative standard deviation of the populations, and (3) an expression for the minimum width of the associated spectral line.

I. INTRODUCTION

As teachers of physics we seek new ways to think about and present the main features of physical systems. We use models and analogies, sometimes even straying into an anthropomorphic mode of expression with phrases such as "...the particles want to get together... ." But beyond these kinds of verbal analogies there may be more developed and complex models arising from nonphysical situations which, when applied to physics, can enhance our understanding of an interest in the phenomenon under consideration. In this paper, we will attempt to demonstrate how the theory of queues (a British word for a file or line of people) can be used to augment our conventional picture of physical processes. The mathematics of queueing can give results identical to those arrived at in the usual way while the particular queue "discipline" or configuration provides an analogy between human processes and physical processes. A physical system which is particularly well adapted to the queue analogy is the two-level system. We will consider two examples of physical two-level systems: (a) radioactive nuclei decaying to a daughter state, and (b) a two-level spin system perturbed by an electromagnetic field. Both systems may be analyzed using the theory of queues. In the case of radioactive decay a time-dependent queue is used and for the two-level system a steady-state approach is taken. The results obtained are identical to those found through the more traditional methods of physics.

II. ELEMENTS OF QUEUEING

The theory of queues is a branch of probability and more specifically forms a subset of the subject of applied stochastic processes.[1] Applications of queueing include not only human queues but also systems analysis (including communications and computers), reliability studies, and other areas usually reserved for engineers with a theoretical bent.[2] In physics and chemistry stochastic processes are widely used although the motivation differs from the queue scenario. Many of the mathematical forms and results of queueing may be found in these other models. However the value of this approach lies in the analogy of the physical process with the easily envisioned human queue.

The queue system consists of the queue itself and some kind of service facility. A typical example would be a doctor's office where the patients in the waiting room are in the queue and the patients being treated by the medical staff are in the service facility. See Fig. 1.

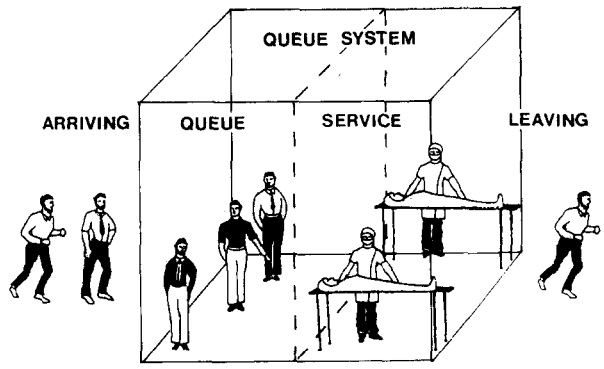

Fig. 1. Queue system for a doctor's office. In general, the queue system consists of both the queue and the service facility. The "service" is provided in this case by the two doctors who have patients on the tables.

 © 1985 American Association of Physics Teachers

This article is copyrighted as indicated in the article. Reuse of AAPT content is subject to the terms at: http://scitation.aip.org/termsconditions. Downloaded to IP: 95.68.109.7 On: Wed, 23 Apr 2014 04:24:23